

FTI Initiative Energy Model Region

Publishable final report

Programme control:

Climate and Energy Fund

Programme management:

The Austrian Research Promotion Agency (FFG)

Final Report

created on

05/11/2022

Project title: EDCSproof

Project number: 868837

FTI Initiative Energy Model Region - 1. Call for Projects

Federal Climate and Energy Fund – Handling by The Austrian Research Promotion Agency FFG

Call	1. Call FTI Initiative Energy Model Region
Project Starting Date	01/10/2018
Project Ending Date	31/12/2022
Total duration of project (in months)	39 Months
Project holder (Institution)	AIT Austrian Institute of Technology GmbH
Contact person	Bernd Windholz
Postal address	Giefinggasse 4, 1210 Vienna
Telephone	+43 664 2351933
Fax	+43 50550-6679
E-mail	bernd.windholz@ait.ac.at
Website	www.ait.ac.at

EDCSproof

Energy Demand Control System -
PROcess Optimization For industrial low temperature systems

Authors:

Bernd Windholz (AIT)
Sophie Knöttner (AIT)
Martin Koller (AIT)
Christoph Zauner (AIT)
Carolin Monsberger (AIT)
Michael Gafert (AIT)
Jaison Puthenkalam (AIT)
Karl-Wilhelm Schenzel (IET)
René Hofmann (IET)
Florian Fuhrmann (ARPA)
Alexander Schirrer (ARPA)
Martin Kozek (ARPA)
Stefan Jakubek (ARPA)
Christoph Sejkora (EVT)
Thomas Kienberger (EVT)
Dominik Riegelneegg (evon)
Martin Sipek (evon)
Gerald Hirschmann (evon)
Christopher Binder (ILF)
Markus Fröch (ILF)
Magdalena Teufner-Kabas (kleinkraft)
Reinhard Teufner (Wiesbauer)
Leopold Sturm (Wiesbauer)
Markus Siedl (Fischer Brot)
Daniel Hager (Fischer Brot)
Stefan Huemer (Fischer Brot)

1. Table of content

1.	Table of content	4
2.	Introduction	6
2.1.	Motivation & starting point	6
2.2.	Consortium	6
3.	Content and Objectives	7
3.1.	Energy Demand Control System (EDCS)	8
3.2.	The challenges for the EDCS	8
4.	Results and conclusions	9
4.1.	Reference energy system	9
4.1.1.	Reference Energy System as innovative holistic energy supply system	9
4.1.2.	Reference Energy System as complementary concept to the EDCS	9
4.1.3.	Laboratory System in the Reference Energy System	10
4.1.4.	Reference Energy System in the Techno Economic Analysis	10
4.2.	High-temperature heat pump	11
4.2.1.	Design and construction	11
4.2.2.	Setup in the laboratory	12
4.2.3.	Measurement results	13
4.2.4.	Conclusions	18
4.3.	Latent heat storage	19
4.3.1.	Phase Change Material	19
4.3.2.	Setup in the laboratory	21
4.3.3.	Measurement results	21
4.3.4.	Conclusions	22
4.4.	EDCS	23
4.4.1.	The solutions implemented in the EDCS	23
4.4.2.	Two-layer optimization: Operation Planner & Model Predictive Controller	23
4.4.3.	Observer	24
4.4.4.	Human-Machine-Interface	24
4.5.	Performance of the EDCS in the laboratory	27
4.5.1.	Introduction	27
4.5.2.	Laboratory setup	27
4.5.3.	Results	29
4.5.4.	Conclusions	33
4.6.	Performance of the EDCSproof concept at the RES	33
4.6.1.	Approach	33
4.6.2.	Results	34
4.7.	Performance of the EDCSproof concept at Wiesbauer Wien	35
4.7.1.	Cost Calculation for the use case Wiesbauer Wien	36
4.7.2.	Cost calculation for the heat pump integration	36
4.7.1.	Cost calculation for the EMS integration	38

FTI Initiative Energy Model Region - 1. Call for Projects

Federal Climate and Energy Fund – Handling by The Austrian Research Promotion Agency FFG

4.7.2.	Economic Analysis	38
4.7.3.	Conclusion	39
4.8.	Applicability of the EDCSproof concept in other industries	39
5.	Outlook and recommendations	40
6.	Bibliography	41
7.	Appendix.....	42
8.	Contact details	43

2. Introduction

2.1. Motivation & starting point

The increasing share of **renewables** in the electric grid leads to increasingly **fluctuating** electricity supply, which demands increasingly **flexible** consumers (demand side management), especially in the **energy-intensive industry**. The manufacturing industry is often not designed for this flexible operation, since storages (electric, thermal, etc.) and (sector-coupling) energy conversion components needed for demand side management (e.g. Power-to-Heat (P2H) preferably by heat pumps for waste heat utilisation) are **not yet standard**. Furthermore, most energy supply systems in industry have **conventional** automation and process control systems. As a result, these control systems are **not operated optimally** (especially not real-time, predictive and holistic) in terms of lowest CO₂ emissions, maximisation of self-consumption of on-site produced energy by renewables, lowest operational costs, etc. At the same time industry **has to reject much heat**, which from a technical point of view could be utilized by high-temperature heat pumps to provide process heat up to 150 °C.

2.2. Consortium

The consortium consisted of the following partners:

Research partners:

- AIT - Austrian Institute of Technology GmbH
 - o Center for Energy
 - o Center for Technology Experience
- Technical University of Vienna
 - o Institute for Energy Systems and Thermodynamics, Working group Industrial Energy Systems (IET)
 - o Institute of Mechanics and Mechatronics, Working group Control and Process Automation (ARPA)
- Montanuniversität Leoben
 - o Chair of Energy Network Technology

Producing Industry:

- Wiesbauer Holding AG
- Fischer Brot GmbH

Engineering, consulting and automation:

- kleinkraft OG
- ILF Consulting Engineers Austria GmbH
- evon GmbH

3. Content and Objectives

The primary goal of **EDCSproof** was developing the online, predictive and holistic, reconfigurable control concept for industrial energy supply systems, which supports the integration of renewables by using (thermal) energy storages (TES), works as flexible consumer for electric grids (demand side management considering dynamic tariffs), increases efficiency by optimal control of the overall system, and utilizes waste heat by using high-temperature heat pumps (HTHP, $< 150\text{ }^{\circ}\text{C}$), hence showing a future concept for decarbonization using the possibilities of digitalization. This also includes a user-friendly human-machine interface (HMI) for efficient input of production plans, visualisation of current and predicted plant states, and possible intervention by operators and managers. The first holistic integration of HTHP and novel TES into the online, predictive control concept needs adequate, fast and accurate simulation models, improved by experimental tests of TES and HTHP. The innovative overall concept was tested and improved in the laboratory for representative use cases. In parallel, the scalability and potential application for other processes and industrial sectors were determined in a techno-economic and ecological assessment.

The expected project result (as part of the NEFI thematic model region) is a widely applicable, cross-sector energy concept for subsequent implementation at the sites of the project partners as well as for a huge majority of companies. The energy efficiency and thus the competitiveness of the producing industry will be increased, the share of renewable energy will be supported, and the pioneering role of Austria strengthened. In addition, plant engineers, automation experts and technology manufacturers will benefit by additional business cases in long term.

EDCSproof was part of the NEFI thematic model region that positions energy intensive and manufacturing industries and their decarbonization in the center of a long-term innovation process to boost technological development. **EDCSproof** contributed to the NEFI-innovation fields Energy Efficiency & New Processes, Renewable Energy & Storage & Demand Side Management, and supported the systemic innovation fields System solutions & Infrastructure, New Business Models.

The project was structured in seven work packages:

1. Project Management and NEFI cluster coordination
2. Know-How Transfer (Dissemination, Claims and IPR)
3. Analysis of partners' plants, definition of reference energy system, objectives, and model requirements
4. Development and modelling of components
5. Operation optimization and automatic control for overall system
6. Setup and testing in the laboratory
7. Techno-economic and ecological analysis and scalability

3.1. Energy Demand Control System (EDCS)

One central solution approach for industry decarbonization is transforming industrial plants into predictable and flexible power consumers. To transform an industrial plant into a flexible consumer, a holistic and predictive energy management system (EMS) has to be developed. The EMS further has to optimize industrial energy supply systems (ESSs) not only in terms of economics but also in terms of efficiency, pollution, machine wear, and flexibility. The method of choice for a predictive optimization-based control system is a model predictive controller (MPC). MPC has been known for decades, and still, the concept of MPC is rarely applied for EMS except for some large industrial plants. Some of the main barriers for a broad application of MPC for EMS are explained in the following. These challenges were the main drivers behind this project and as one of the main results: the development of the energy demand control system (EDCS).

3.2. The challenges for the EDCS

High implementation costs due to the modelling effort: The first major challenge is that building effective models for model-based controllers, as MPCs, is a difficult task. It typically requires considerable effort by specialists and elaborate data-based validation to derive a valuable model of the relevant plant dynamics. The challenge is intensified due to the grown and individual structures of ESS in industrial plants. Furthermore, ESSs are frequently adapted to implement renewable energy sources or to react to changes in the production process. The modelling process must be repeated at each significant change or upgrade of the ESS and for each new plant.

Human interactions: The usually semi-automated nature of industrial production processes causes multiple human-machine interactions. Predictions of these interactions are challenging and rarely made in practice. Thereby the human interactions become unpredicted disturbances to the control system and hinder an optimal operation of the ESS.

High computational effort: High computational effort is caused by two reasons: the combinatoric nature of the optimization problem, resulting in mixed-integer formulations, and the long prediction horizon. The unit commitment decisions require integer decision variables in the optimization problem causing (potentially) high calculation effort in optimization. The prediction horizon is determined by the time schedule of the power market. To exploit the modern power market, power consumption needs to be known about 24 hours in advance. Furthermore, the actual power consumption needs to follow the predicted one for each 15-minute. Due to that and production safety, the sampling time is favourably chosen approximately one minute. The combination of mixed-integer optimization, 24h prediction interval and short sampling times results in enormous calculation effort.

Uncertainties of predictions: Uncertainties of disturbance predictions like load predictions or weather predictions have a crucial impact on the MPC performance [1]. Especially, the load prediction is challenging as it strongly depends on the production plan, which is subject to short-term changes. Furthermore, the above-mentioned semi-automated production process causes deviations from the planned time schedule. These uncertainties do not just affect control performance but can also cause bottlenecks in the energy supply and thereby impact production reliability.

4. Results and conclusions

In the following, the main publishable results of the project are presented.

4.1. Reference energy system

The Reference Energy System (RES) is a holistic industrial energy supply system for supplying all load requirements in low temperature processes $<150\text{ }^{\circ}\text{C}$. In order to investigate all possibilities for flexibilization and decarbonization of industrial consumers, the RES is a combination of currently common supply systems and technological innovations such as (high-temperature) heat pumps (HT(HP)) and storages (thermal and electrical) to improve the utilization of waste heat and renewable sources.

4.1.1. Reference Energy System as innovative holistic energy supply system

The holistic integration of different individual components and systems is one of the core issues and main innovations in the project EDCSproof. All individual components are considered and combined in a single RES to be able to cover all load requirements in the low-temperature processes up to $150\text{ }^{\circ}\text{C}$ in a highly efficient way. This promising systemic approach has not yet been investigated, as some of the technologies are still in the development or demonstration phase (TRL4-5). As a basis for the development of a suitable design of the RES, various sources of information were considered:

- Literature search on energy sources in the Austrian food sector,
- Analysis of the processes of the three industrial project partners' use cases
- Findings from the variety of preliminary projects where mainly new innovative supply technologies and concepts were analysed.

To give the RES a viable character, also a reference-energy-demand scenario was defined together with the RES. Based on this scenario, the individual components of the RES were dimensioned in terms of their size, power and capacity using a design optimization model.

4.1.2. Reference Energy System as complementary concept to the EDCS

By the common interaction of individual technologies and components, both advantages can be strengthened and disadvantages can be compensated. For example, HPs are very efficient and particularly suitable for waste heat utilisation. For economical operation, HPs need to be run at a specific minimum amount of full load hours. This may be a challenging task, especially if waste heat utilisation has to be applied to batch processes. Here, thermal storages (TES) can ensure continuous operation and high full load hours by smoothing the load for the HP. In addition, the economic performance of the TES gets improved if more storage cycles are achieved. With rising complexity more components work together and such symbiotic potentials are increasing. Nonetheless, for such complex energy systems, the effort for process integration and advanced process control systems increases extremely.

Diversified supply systems can only be fully exploited and optimized through the application of innovative, holistic and predictive operating strategies and control systems. Hence, it makes particular sense to develop the concepts of RES and EDCS together. In the combined development approach, the RES serves as a virtual test case for the development and functional testing of the EDCS.

4.1.3. Laboratory System in the Reference Energy System

Once the innovative overall concepts were developed and virtually tested, the EDCS was tested in a laboratory environment on a simplified system consisting of a HP and TES for achieving a higher technological readiness level. The laboratory system can be found as a HTHP and latent storage in the RES.

4.1.4. Reference Energy System in the Techno Economic Analysis

In the techno-economic analysis the developed concepts are comprehensively and complementary assessed. The RES takes on an essential role as it is used as a test case for the analysis of several investment and operation scenarios.

Based on the findings of the analyses and studies as well as corresponding coordination within the project team, the configuration shown in Figure 1 was developed as RES. While this system does not fully represent any of the individual use cases in total, it is a reasonable extensive overlap. However, by setting different limits, parameters and switching of non-essential components, all significant subsystems of the use cases can be recreated. In addition, this RES also considers innovative technological design optimizations (HP, TES, renewable suppliers) to be able to carry out and analyze process and efficiency improvements.

FTI Initiative Energy Model Region - 1. Call for Projects

Federal Climate and Energy Fund – Handling by The Austrian Research Promotion Agency FFG

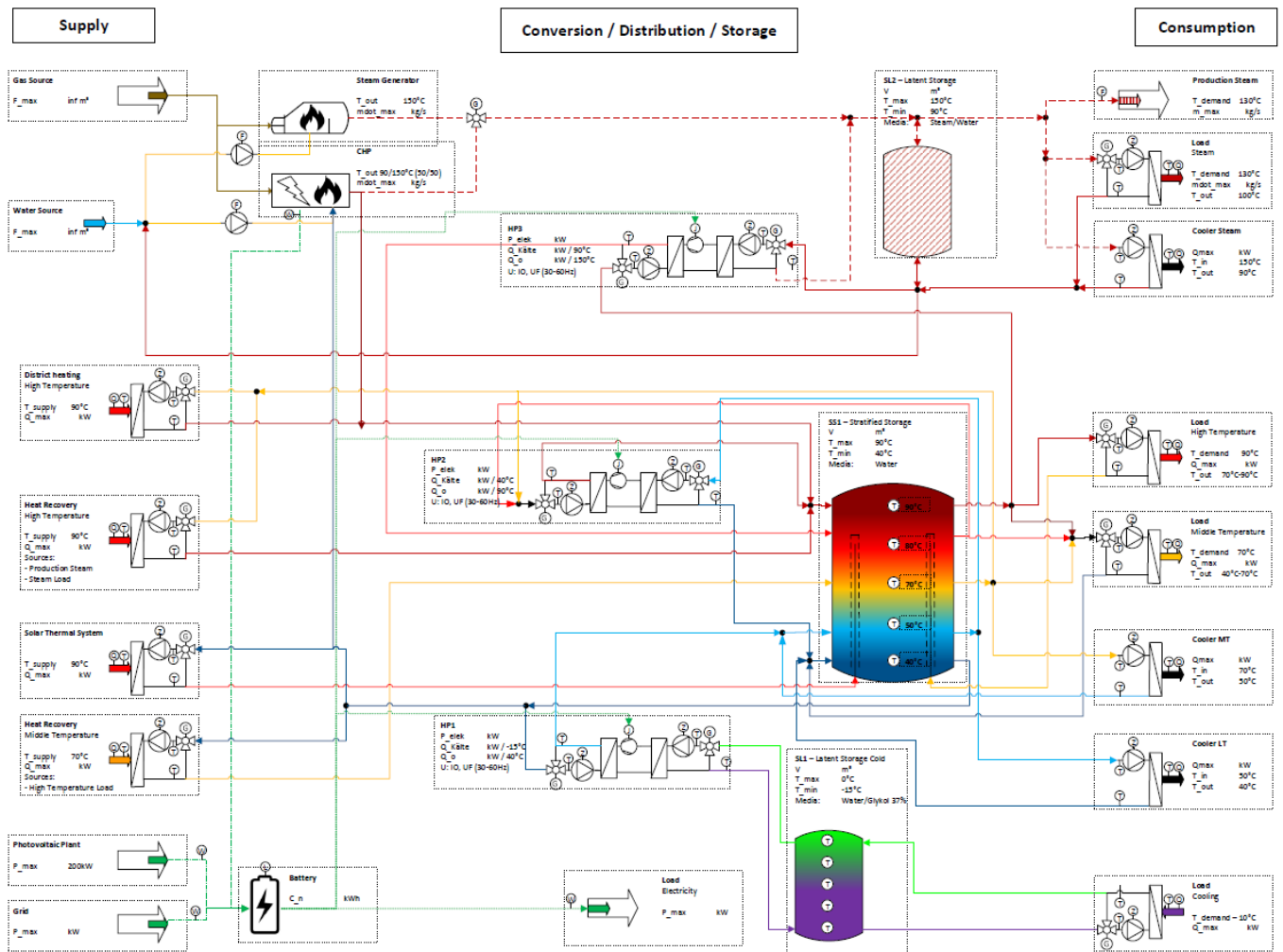


Figure 1: Reference energy system

4.2. High-temperature heat pump

For the development of the EDCS and having it tested in the lab, models of (high-temperature) heat pumps ((HT)HP) were necessary. For this purpose the existing HTHHP system “High Butane 2.0” – designed for an industrial application– was rented from Frigopol Kälteanlagen GmbH. It was set up and tested in the AIT HP laboratory.

4.2.1. Design and construction

The HP was developed by AIT, SINTEF and Frigopol within “High Butane 2.0” (FFG project no.: 843935). An overview of Arpagaus about HTHPs shows that a big share of industrial processes up to 100 °C can be supplied via state-of-the-art HP technology. Currently, HTHPs up to 160 °C are developed. Schmid et al. [2] introduced butane as advantageous refrigerant for temperatures above 100 °C, since its critical temperature is higher compared to other hydrocarbons and at the same time the volumetric refrigeration capacity is high while the global warming potential is low (GWP = 4). Since butane is easily flammable, the filling quantity and installation site have to be chosen carefully. Out of this work, a HTHP (water/water) was built. The HP contains 12 kg n-Butan (R600) as refrigerant and an ejector in the refrigeration cycle, see

Figure 2. This HP can switchable be operated without ejector and was designed for: heating capacity: 50 kW, temperature lift on heating side: 100 to 130 °C, inlet temperature on the cooling side: 60 °C.



Figure 2: n-butane high-temperature heat pump with opened housing. Source: Frigopol Kälteanlagen GmbH

The demonstration of the HTHP in an industrial extrusion factory within StoreITup-IF (FFG project no. 848914) showed, that the HP prototype can be optimized, see Zauner et al. [3]. Schlemminger et al. [4] analysed the measurement values with a focus on the ejector and concluded, that further tests are necessary.

4.2.2. Setup in the laboratory

The HP was set up in the insulated and tempered climate chamber for HPs with a liquid heat source in AIT's HP laboratory, see Figure 3. At the evaporator of the HP, heat is extracted from the test bench. In the HP the condenser is connected to a water circuit, which is cooled by the test bench (heat sink). The heat source and heat sink are conditioned by the test bench, see Figure 4.



Figure 3: High-temperature heat pump in a climate chamber of AIT's heat pump laboratory

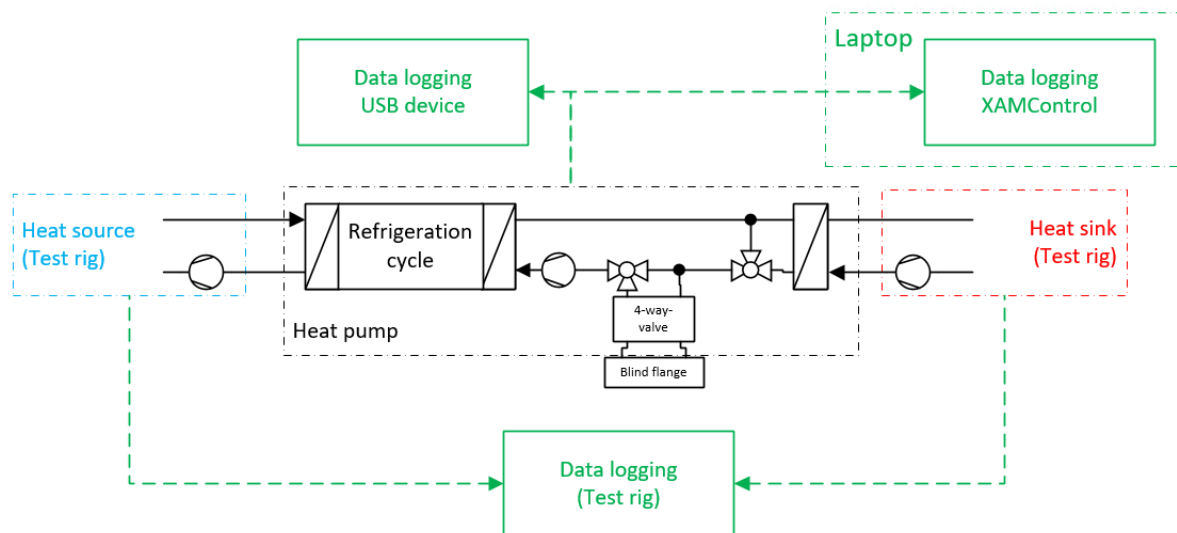


Figure 4: Setup of the heat pump (centre, black) in the test rig (left and right, blue and red) and the data logging (green)

Since the HP is controlled by many actuators, e.g., the speed of the compressor, a proper characterization depends on values of these actuators' states. For the characterization and subsequent modelling of the HP, important parameters and measurement values were made accessible for datalogging. Data logging and the connections are shown in Figure 4.

4.2.3. Measurement results

Measurement data were recorded from about 12 operating days, of which about 8.5 days were evaluated. The HP was tested at different source/sink temperatures and -flow rates, the setpoints of the HP were set to different values. During operation, the controlled variables sometimes showed oscillating behaviour. This shows that the control parameters of the individual controllers still need to be optimized. Accordingly, operation was frequently unsteady, which led to difficulties in the result evaluation and interpretation. The evaluations were therefore elaborated with 5- minute mean values Furthermore, in some cases only almost stationary conditions could be realized.

The sensors of the test rig are regularly calibrated to maintain the accreditation of the laboratory, therefore their measurement uncertainty is correspondingly low. This concerns the electrical power as well as temperatures and mass flows of the heat source and -sink. The measurement uncertainty of the sensors of the HP corresponds to the manufacturer's specifications. This concerns the states (pressures, temperatures) of the n-butane in the refrigeration circuit as well as temperatures and flow in the intermediate water circuit at the condenser. The measurement data evaluation was done with the help of the programming language python¹, state variables such as density and specific enthalpy of the media (n-butane, water) were determined from the measured data using CoolProp, an opensource library for thermophysical properties.² [5]

¹ Programming language Python: www.python.org

² Open-source library for thermophysical properties of materials CoolProp: www.coolprop.org

4.2.3.1. Suction gas superheating, losses

The heat exchanger for the suction gas superheating is oversized, which is another reason why a bypass is provided so that the superheating can be controlled with a three-way valve. Due to the thermal mass, the superheating reacts very sluggishly to changes in the control variable, so that the actual superheating depending on the setpoint often assumes values that are significantly too high. In this case, the compressor speed is automatically reduced for safety reasons. As a simple remedy, the HP case was opened, and cooling of the chamber was activated.

The HP’s power loss results from its power balance:

$$\dot{Q}_V = |\dot{Q}_{\text{evap}}| + |P_{\text{el}}| - |\dot{Q}_{\text{cond}}| \tag{1}$$

The power loss \dot{Q}_V is the sum of the supplied heat power on the source side \dot{Q}_{evap} and the electrical power P_{el} minus the dissipated heat power on the sink side \dot{Q}_{cond} . If the power loss is related to the sum of the supplied powers, the result is the so-called balance error, which is on average about 8 % for this HP. This value is comparatively low compared to many other measurements carried out on this test rig, although the HP was operated at higher temperatures and with the casing mostly open and therefore higher losses were expected.

4.2.3.2. Heating capacity and second-law efficiency

For the evaluation of the heating power and the second-law efficiency, 5-minute averages were formed, and comparatively stationary conditions were selected. The data evaluation shows that the heating power tends to increase with increasing sink outlet temperature, see Figure 5, but it also depends on other parameters, especially the source outlet temperature and the temperature difference at the condenser. The values of these parameters can be read in the diagram by means of the colour or the symbol. The data shown are valid for the maximum compressor speed and a maximum superheating after the evaporator of 15 K. Suction and hot gas superheating are higher than intended at an average of 21 and 14 K, respectively. Numerical values for the diagram can be found in Table 8.

The highest heating power shown is 31 kW with sink heating from 97 to 107 °C and source cooling from 51 to 41 °C. The highest depicted sink outlet temperature of 112.6 °C is obtained with source cooling from 50 to 47 °C and a heating power of 29 kW. In each case, the source and sink temperatures deviate significantly from the design conditions (50 kW at sink 100/130 °C and source inlet temperature 60 °C), so a comparison of the actual measured data with the design data is not meaningful.

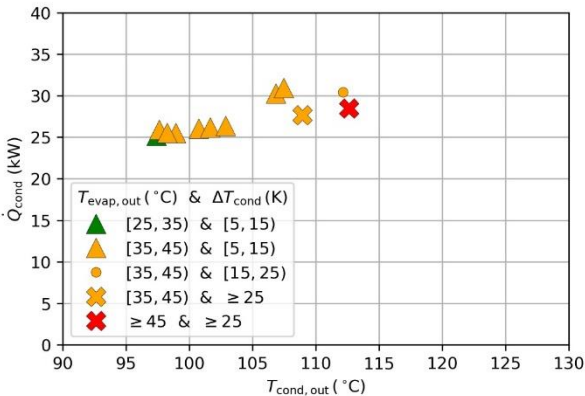


Figure 5: Heat pump heating capacity depending on the sink outlet temperature with the source outlet temperature and the temperature difference at the condenser as parameters, see Table 8

If the heating capacity is related to the power consumption of the HP, the coefficient of performance (COP) is obtained:

$$\text{COP} = \frac{|\dot{Q}_{\text{cond}}|}{|P_{\text{el}}|} \quad (2)$$

The coefficient of performance of a Carnot process operating between two constant temperature levels for heat supply and removal (temperatures in K) is given by:

$$\text{COP}_C = \frac{T_{\text{ab}}}{T_{\text{ab}} - T_{\text{zu}}} \quad (3)$$

The second-law efficiency of the HP is obtained by comparing the achieved coefficient of performance with the maximum achievable coefficient of performance of a Carnot process operating between the evaporating and condensing temperature levels:

$$\eta_c = \frac{\text{COP}}{\text{COP}_C} \quad (4)$$

Figure 6 shows the second-law efficiency of the HP as a function of the heating power. It is in the range of 0.39 to 0.42 at the observed partial load of 25 to 31 kW (design power is 50 kW) and increases slightly with increasing heating power. Numerical values for the diagram can be found in Table 8.

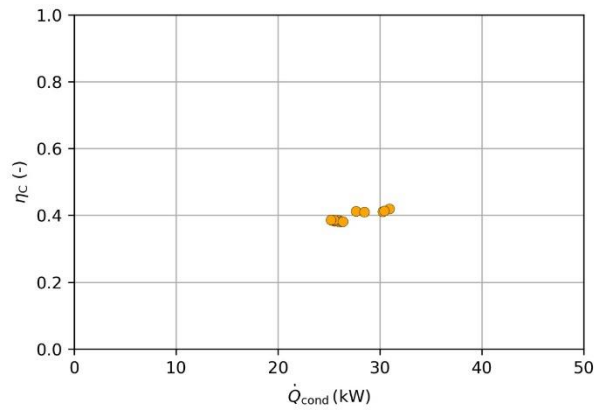


Figure 6: Second-law efficiency of the heat pump depending on of the heat output, see Table 8

4.2.3.3. Ejector

The characterization of the ejector is done analogously to Schlemminger et al. [4] with different parameters. The entrainment ratio of the ejector is defined as the ratio of the entrained low-pressure mass flow to the driving high-pressure mass flow:

$$M_{\text{ej}} = \frac{\dot{m}_{\text{nd}}}{\dot{m}_{\text{hd}}} \quad (5)$$

The pressure ratio of the ejector is the medium pressure reached at the outlet in relation to the low pressure:

$$\Pi_{\text{ej}} = \frac{p_{\text{md}}}{p_{\text{nd}}} \quad (6)$$

The correlation between the entrainment ratio and the pressure ratio determined from the measured data is shown in Figure 7 with high pressure as the coloured parameter. The entrainment ratio tends to decrease with increasing pressure ratio. The highest entrainment ratio of 0.86 and thus the lowest pressure ratio of about 1.20 were observed at a high pressure of 14.3 bar. The highest pressure ratio of 1.41 and thus the lowest entrainment ratio of just above 0.45 were observed at a high pressure of 21.2 bar.

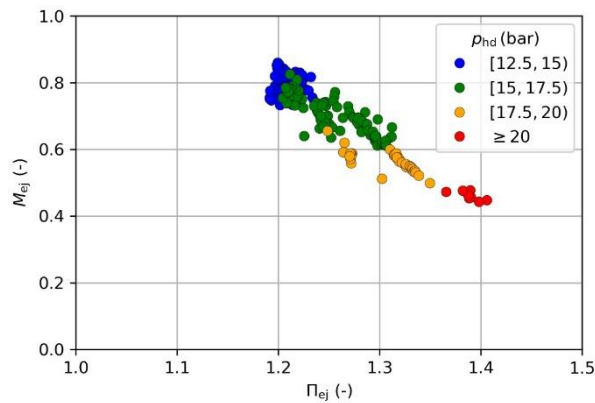


Figure 7: Entrainment ratio as a function of the pressure ratio with the high pressure as parameter

The ejector efficiency calculated by Schlemminger et al. [4] according to Elbel and Lawrence [6] is defined as

$$\eta_{ej} = M_{ej} \frac{h(p_{md}, s_{hd}) - h_{hd}}{h_{hd} - h(p_{md}, s_{hd})} \quad (7)$$

It is the ratio of the work recovered in the ejector during compression of the low-pressure mass flow to the maximum possible expansion work of the high-pressure mass flow during isentropic change of state.

The correlation between ejector efficiency and pressure ratio obtained from the measured data is shown in Figure 8. There is some correlation with the heating power, which is shown in colour in the diagram. There is a tendency for the ejector efficiency to decrease with increasing pressure ratio and with increasing heating power. The highest ejector efficiency of 0.56 was observed at a pressure ratio of 1.20. The lowest ejector efficiency of 0.33 were observed at a pressure ratio of 1.41.

The current measurements allow characterization of the ejector over a wide operating range. This also reproduces the measurement point ($\Pi_{ej} = 1,36$, $M_{ej} = 0,46$ und $\eta_{ej} = 0,35$) studied by Schlemminger et al. [4]: $\Pi_{ej} = 1,37$, $M_{ej} = 0,47$ und $\eta_{ej} = 0,34$.

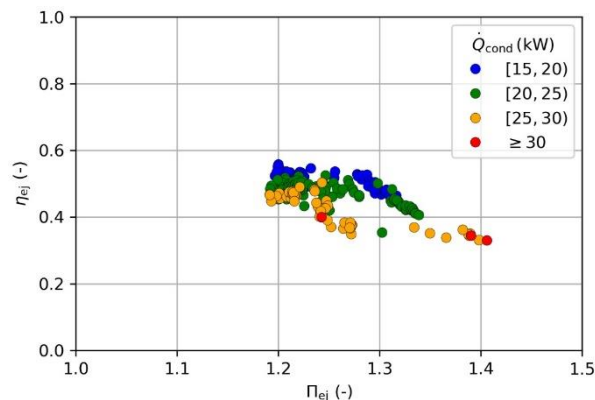


Figure 8: Ejector efficiency depending on the pressure ratio with the heating power as parameter

4.2.3.4. Compressor

To characterize the compressor, 5-minute averages were taken, and comparatively steady states were selected.

The pressure ratio of the compressor is the ratio of the outlet pressure to the inlet pressure:

$$\Pi_{\text{compr}} = \frac{p_{\text{HG}}}{p_{\text{SG}}} \quad (8)$$

Isentropic efficiency is defined as the ratio of the compression work at isentropic state change to the actual compression work:

$$\eta_s = \frac{h_{s,\text{HG}} - h_{s,\text{G}}}{h_{\text{HG}} - h_{\text{SG}}} \quad (9)$$

The observed isentropic efficiency of the compressor at maximum speed ranges from 0.76 to 0.91. It decreases with increasing pressure ratio, as shown in Figure 9. As expected, the isentropic efficiency correlates with the ambient temperature of the compressor, which is shown in colour in the graph.

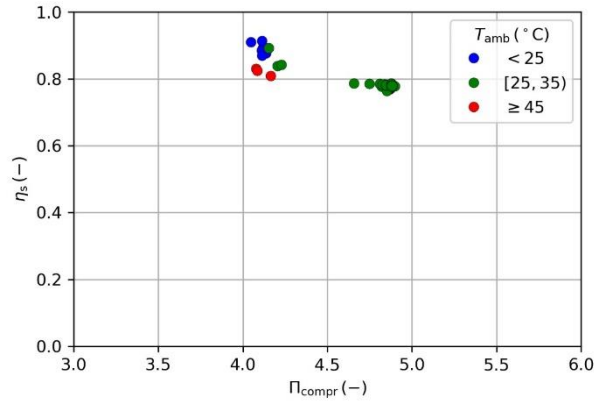


Figure 9: Isentropic efficiency of the compressor at different pressure ratios and different ambient temperatures

The compressor efficiency is the enthalpy increase of the pumped mass flow between compressor inlet and outlet related to the electrical power supplied to the compressor:

$$\eta_{\text{compr}} = \frac{\dot{m} \cdot (h_{\text{out}} - h_{\text{in}})}{P_{\text{el}}} \quad (10)$$

Due to the existing measurement technology, the system boundary is extended so that the oil circuit is within the system. The mass flow that is conveyed through the condenser is used - ideally pure refrigerant. This neglects the oil that is also transported through the compressor, which is separated from the refrigerant in the oil separator and returned to the compressor. The power consumption of the entire HP is considered here. However, most of it is the power consumption of the compressor. This approach underestimates the actual grade of the compressor and thus represents a lower bound.

The lower bound of the compressor quality at maximum speed determined in this way lies between 0.42 and 0.60. A clear dependence on the pressure ratio cannot be determined on the basis of the measured data, see Figure 10. However, there is a correlation with the condensate mass flow, which is highlighted in colour in the diagram.

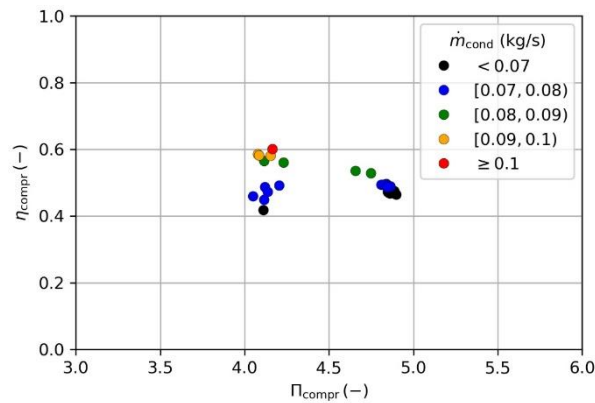


Figure 10: Lower limit of the compressor efficiency at different pressure ratios and different condenser mass flows

The volumetric efficiency of the compressor is the ratio of the delivered mass flow to the geometrically maximum possible mass flow. The maximum value results from the geometrically given volume flow at a given speed and the density of the refrigerant at the compressor inlet:

$$\Lambda = \frac{\dot{m}}{\dot{m}_{\max}} \quad (11)$$

As in the case of limiting the compressor efficiency, the mass flow rate that is conveyed through the condenser - ideally pure refrigerant - is also used for the volumetric efficiency. This approach underestimates the actual volumetric efficiency of the compressor and thus represents a lower bound.

The observed compressor volumetric efficiency at maximum speed ranges from 0.48 to 0.68, shown in Figure 11. There is a tendency for the degree of delivery to decrease as the pressure ratio increases - however, the wide spread of the points shown indicates that the pressure ratio is not the only determining variable.

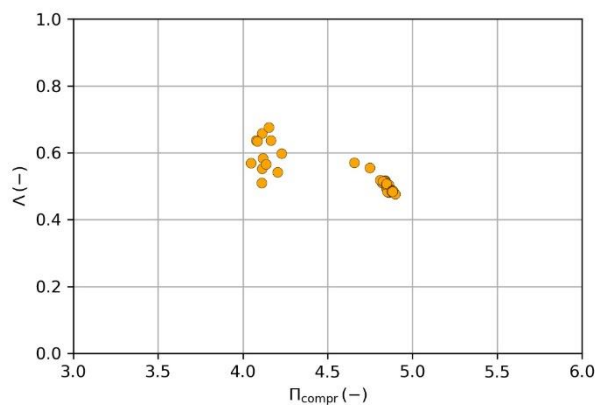


Figure 11: Lower limit of the volumetric efficiency of the compressor at different pressure ratios

4.2.4. Conclusions

The evaluation of the measured data shows that operation was relatively dynamic despite uniform source and sink states. One main reason for this is the still open optimization of the individual controllers of the HP and, moreover, their interaction, so that the setpoints of the controlled variables are more reliably and

stably adjusted and the manipulated variables settle to stationary values. This prerequisite should be fulfilled before further measurements.

Due to the thermal inertia of the suction gas superheater, this also applies to the control of superheating, which, depending on the setpoint, assumes values that are significantly too high, as a result of which the compressor speed is automatically reduced for safety reasons.

The source and sink temperatures conditioned during the measurements deviate significantly from the design conditions (50 kW at sink 100/130 °C and source inlet temperature 60 °C), a comparison of the current measurement data with the design data is therefore not reasonably possible and requires further measurements.

The current measurement results allowed the characterization of the HP, especially the ejector and the compressor, over a wide operating range based on various parameters. The presented results provide valuable correlations for the modelling of the heat pump and model validation. Furthermore, the measurement results were an important building block for the further development and improvement of the HP.

4.3. Latent heat storage

For the development of the EDCS among others models of latent heat storages were necessary. The latent heat storage technology was improved – a storage was derived and technically designed. Existing models from AIT were used to design the storage. The storage tank was set up and tested in the AIT thermal storage laboratory.

4.3.1. Phase Change Material

First, a survey for possible material candidates was performed. Phase Change Materials (PCMs) have to fulfil a number of criteria to be viable for large-scale industrially manufactured and globally available PCM storages at reasonable costs. Thus, a list of criteria was defined, described in the following subsections:

4.3.1.1. Phase Change Temperature

The interesting phase change of the PCM storage within this project was initially defined to be in the range of 100-200 °C. Later this range was narrowed down to be compatible with the foreseen hardware of the lab set-up. In general, PCMs melt and solidify within certain temperature ranges (and not “phase change points”), which are usually different. In real-scale storages, the actual ranges depend quite a lot on sample size and geometry as well as substance purity, container material properties (e.g., roughness) and also temperature gradients during melting and solidification. One has to keep this fact in mind when choosing PCMs and interpreting available data, which often stems from lab measurements of very small samples (grams, cubic-centimetres). The situation in a real-scale storage (tons, cubic-meters) is often much different and especially large-subcooling (difference between melting and solidification) sometimes observed in lab-DSC-measurements (Differential Scanning Calorimetry) is much less present in real applications.

4.3.1.2. Phase Change Enthalpy

The phase change enthalpy of a substance can be defined with regard to its volume (volumetric) or mass (gravimetric). Depending on the application, one of them or even both might be relevant. In this project, we screened all candidate PCMs with at least 100 kJ/kg in a first step and focused on organic PCMs. Nitrate salts are already well studied and suitable for various applications and storage designs but have not been studied in this project in more depth.

4.3.1.3. Price Indication, Bulk Availability

The most relevant factor for companies to invest or not invest in energy saving or carbon neutral production technologies is the economic feasibility. The return-on-investment usually has to be less than 5 years, very often 3 years and rarely longer. Using a PCM storage, allows saving energy and money by storing solar heat or waste heat and re-use it later. With low gas and CO₂ prices (e.g. Q2 2020), it is only possible to design ultra-cheap PCM storages using very cheap PCMs. Although, we also screened materials that might only be relevant in a future “no-fossil world”, PCM costs are a very relevant figure, which we tried to pin down for future large scale (multi-ton) applications.

The lab storage was meant to be in the 100 kg PCM range to be large enough to cover all relevant physical effects that would also occur in a fully industrial multi-ton storage. However, if PCM storages are ever meant to play a significant role in industry worldwide, global availability of PCM candidate materials at large scale is important. We studied some candidates, which are already being produced in such a way (e.g., polymers), but also incorporated material that can be mass-produced in the future using known organic chemistry and chemical engineering techniques (e.g., reactors).

4.3.1.4. Toxicity, Processability, Handling:

Although a PCM storage is a special technical apparatus that will be operated in a dedicated industrial environment, which is used to handle a variety of chemicals, one has to keep an eye on the MSDS (Material Safety Data Sheets) when it comes to storage manufacturing, maintenance, operation and end-of-life.

4.3.1.5. Thermal Stability

Future PCM storages will have to be operated for years and most likely thousands to ten-thousands of charging (melting) and discharging (solidification) cycles. The storage material is kept at the molten state for at least a few hours every day in most applications. Most candidate materials have not been designed for such high temperatures and for almost none of them any information on long-term stability under such harsh conditions is available. Thus, we conducted dedicated hot plate experiments. The simplest and thus cheapest PCM storage concepts do not employ special protection measures like inert atmosphere e.g., thus the hot PCM is in direct contact with hot air (oxygen).

4.3.1.6. Compatibility with Heat Exchanger and container

We use heat exchangers to transfer heat from a heat transfer medium to the PCM (and vice versa). Different designs are feasible in principle, e.g., fin-tube, plate, tube bundle, which can be manufactured of a variety of materials and material combinations. In order to minimize costs, we focus on steel and aluminium alloys. The storage container itself was also made of a stainless steel alloy. Both heat exchanger and container are in permanent contact with the hot PCM and also have to be durable for years. Thus, especially corrosion is an important issue that has to be investigated. Unfortunately, for most candidate PCM no data on long-term behaviour and possible degradation is available at the relevant conditions, which is why we also set up dedicated experiments.

4.3.2. Setup in the laboratory

The storage was set up in AIT's thermal storage lab and connected to a thermostat, see Figure 12. Via a thermal oil cycle, the storage can be heated up and cooled down to defined temperatures. Before about 1000 kg of the PCM was filled into the storage, the storage was insulated, and temperature sensors were placed inside. Repeated melting and solidifying were necessary for complete filling due to cavities within the PCM.



Figure 12: Latent heat storage (not insulated) connected to a thermostat in AIT's thermal storage laboratory

4.3.3. Measurement results

With the latent heat storage 16 experiments were performed in the AIT thermal storage laboratory within roughly 2 weeks. These include charging and discharging with constant mass flow of ca. 0,25 kg/s and

- (i) constant inlet temperatures (step answers) with target temperatures ranging from 108 °C to 193 °C (phase-change at ca. 168 °C) as well as with
- (ii) constant power (variable inlet temperatures) with a range from -10 to 10 kW by permanent automatically adapting the thermostat's setpoint of the storage inlet temperature.

In the following, exemplary measurement results for one storage charging and one storage discharging situation is presented. In Figure 13 one can see the power profile (brown; right axis), total stored energy (green; right axis), inlet/outlet temperatures (red, blue; left axis), and PCM temperatures (cyan, light green, olive; left axis) for charging the storage from 128 °C to 188 °C with a constant mass flow of 0.24 kg/s (black; left axis). A comparison with simulation data revealed that the model overestimated the storage charging power. A similar situation arises when comparing the simulation results of a discharging example from 188 °C to 108 °C with a mass flow of 0.23 kg/s (Figure 14). A possible explanation for the deviation of experiment and simulation stems most likely from the wrong assumptions that convection can be neglected in this very PCM. However, in order to perform a quick dimensioning of such a PCM storage, the developed Modelica models are suitable.

FTI Initiative Energy Model Region - 1. Call for Projects

Federal Climate and Energy Fund – Handling by The Austrian Research Promotion Agency FFG

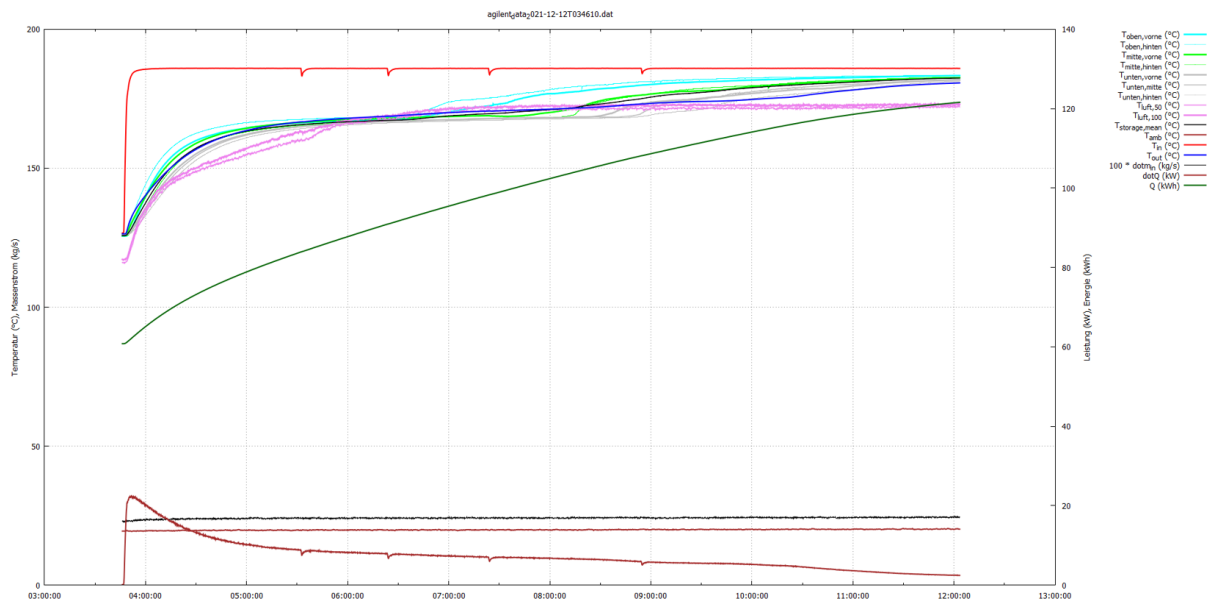


Figure 13: Charging of the PCM lab storage for a specific temperature and mass flow example – experimental results.

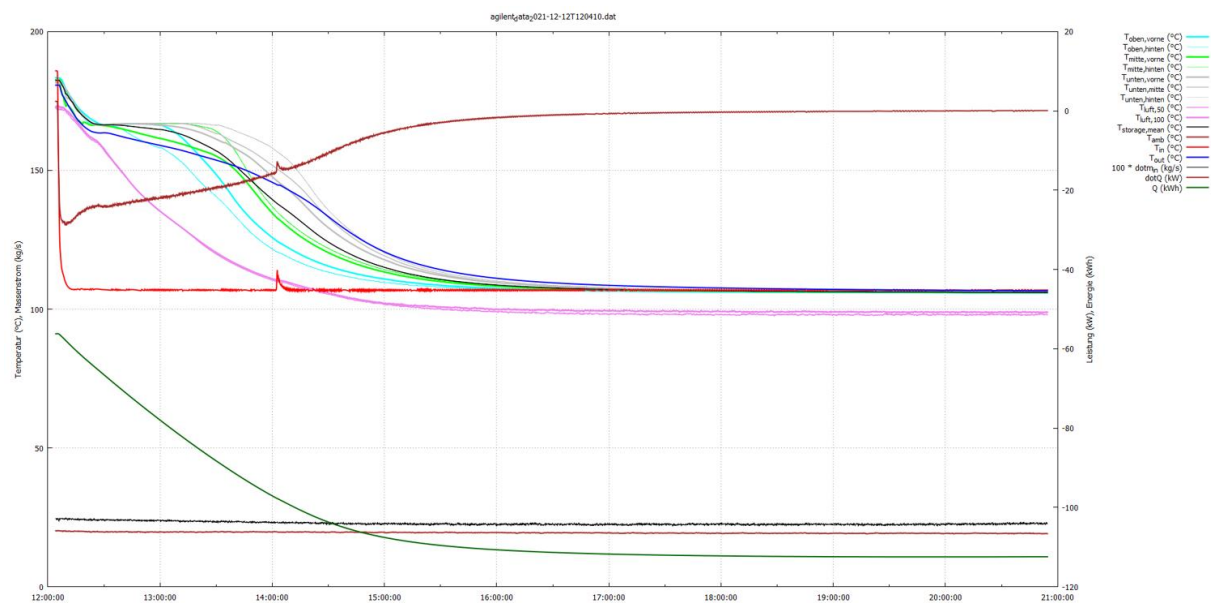


Figure 14: Discharging of the PCM lab storage for a specific temperature and mass flow example – experimental results.

4.3.4. Conclusions

The experiments successfully showed the capacity and behaviour of the latent heat storage during different step answers and constant power tests. Regarding modelling, it has to be stated that the Dymola/Modelica 1-dimensional model has limitations and deviations between experiment and simulations occur. An unclarified question after EDCSproof regarding the PCM storage concerns its long-term stability. Thus, the efforts will be continued in the NEFI project envloTcast³ with a long-term durability test of this

³ <https://nefi.at/en/project/enviotcast>

ECDSproof storage, beginning at the AIT thermal storage lab. Within the EU project HyCool⁴, two similar storages are currently tested in real industrial applications and proof that the technology is almost market ready.

4.4. EDCS

4.4.1. The solutions implemented in the EDCS

The challenges presented in section 3.2 were the main drivers for the development of the EDCS. The resulting structure of the EDCS is displayed in Figure 15, consisting of four main components: the Human-Machine-Interface (HMI), the observer, the operation planner (OP), and the MPC. The OP and the MPC represent a two-layer model-based optimal controller. They are solving mixed-integer linear programs (MILPs) that consist of constraints which ensure that all operation points lie within the process and market boundaries as well as objectives to quantify and optimize the control performance. To reduce the implementation effort, a generic implementation method was developed. It enables a component-wise definition of constraints and objectives and a straightforward parameterization. The HMI is responsible for transforming human interaction into changes of constraints and objectives and making these disturbances manageable and predictable for the EDCS. The observer utilizes the production plan and measurement data to reduce the adverse effects of uncertainties in predictions. In the following subchapters, the components are described more precisely as far as possible due to pending patenting and publication processes.

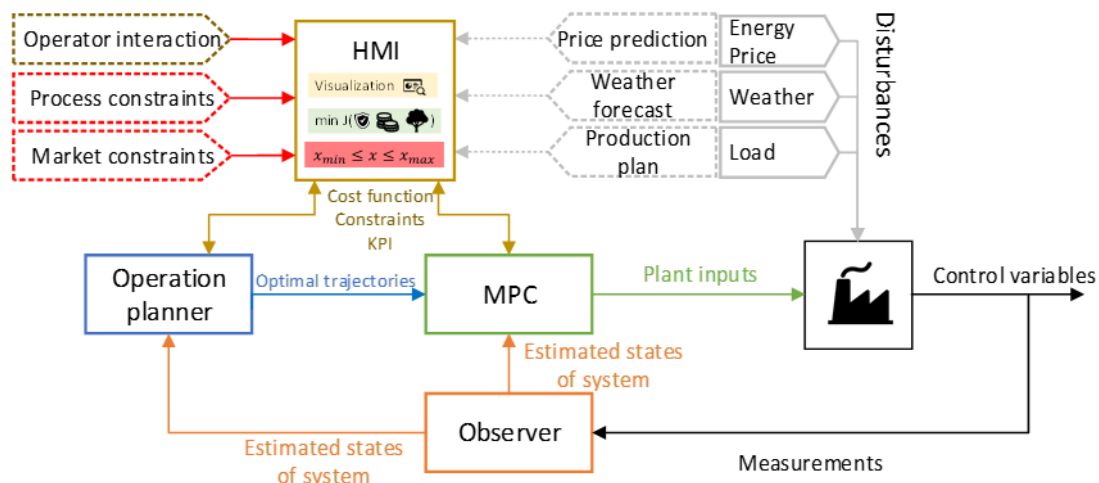


Figure 15: Structure of the EDCS

4.4.2. Two-layer optimization: Operation Planner & Model Predictive Controller

The OP and the MPC or the structure of the MILP solved by them, respectively, tackle two challenges: the **high computational effort due to the modeling effort** and the **high implementation cost**. To enable a generic and fast utilization of the EDCS, the MILP is built component-wise. This further enables a fast adaption to changes of the ESS. In the two-layer optimization, the OP considers the long-term effects with a sampling time $t_{s,HLC}$ of 15 minutes while the MPC is responsible for short-term effects, with a prediction

⁴ <https://hycool-project.eu/>

horizon $N_{P,LLC}$ of a few hours and a sampling time of one minute. This enables an actual time application of the EDCS.

4.4.3. Observer

The measuring equipment installed in ESSs is insufficient to measure all crucial states for optimal control directly. The observer estimates those thermodynamic states of the ESS, like the state of charge (SOC) of energy storages. Further, it utilizes measurement data to correct the load predictions. Thereby the effect of **uncertainties of the predictions** can be reduced. A special focus was laid on batch processes as they are especially challenging for EMS. A load prediction model was developed and included to the observer to enable online load prediction [7]. Further guidelines for model predictive control dealing with uncertain pulse-like disturbances caused by human operators were developed and published [8].

4.4.4. Human-Machine-Interface

The HMI shall provide an interface for the operators to:

- announce and plan their interactions with the ESS
- import prediction plans
- visualize the current status of the ESS
- visualize the anticipated actions and the performance of the EDCS

Thereby the **human interactions** become predictable for the EDCS, and the negative impact on the control performance is mitigated.

Through data acquisition of the industrial plants and discussion with the partners, user stories were defined for each possible interaction with the EDCS. Each user accesses different functionalities of the optimizer and therefore has a different HMI allowing the required access to the optimizer. The user stories were evaluated by the industry partners. Based on the feedback the HMI focuses on the plant operator of the energy consumers and the plant manager.

Based on the user stories generated, an HMI concept was designed. These designs provide the features which are necessary to pass the required information to the OP and the MPC, Figure 15. The four developed use-cases are:

- (i) **Manager** (top-level view of KPIs, optimization parameters and their change over time),
- (ii) **Plant operator of the production facilities (energy consumers)** (creation of production plans, checking of production)
- (iii) **Plant operator of the energy supply system** (Implements the optimizations based on the EDCS for energy supply units which are not automatically controlled)
- (iv) **Technician** (information about disturbances of the energy supply units).

Conceptual HMI designs for the plant operator of the production facilities and the technician are shown in Figure 16 and Figure 17. More extensive HMI concepts of the manager are shown in Figure 18, Figure 19, and Figure 20.

FTI Initiative Energy Model Region - 1. Call for Projects

Federal Climate and Energy Fund – Handling by The Austrian Research Promotion Agency FFG

EDCSProof Anlagenfahrer der Energieverbraucher

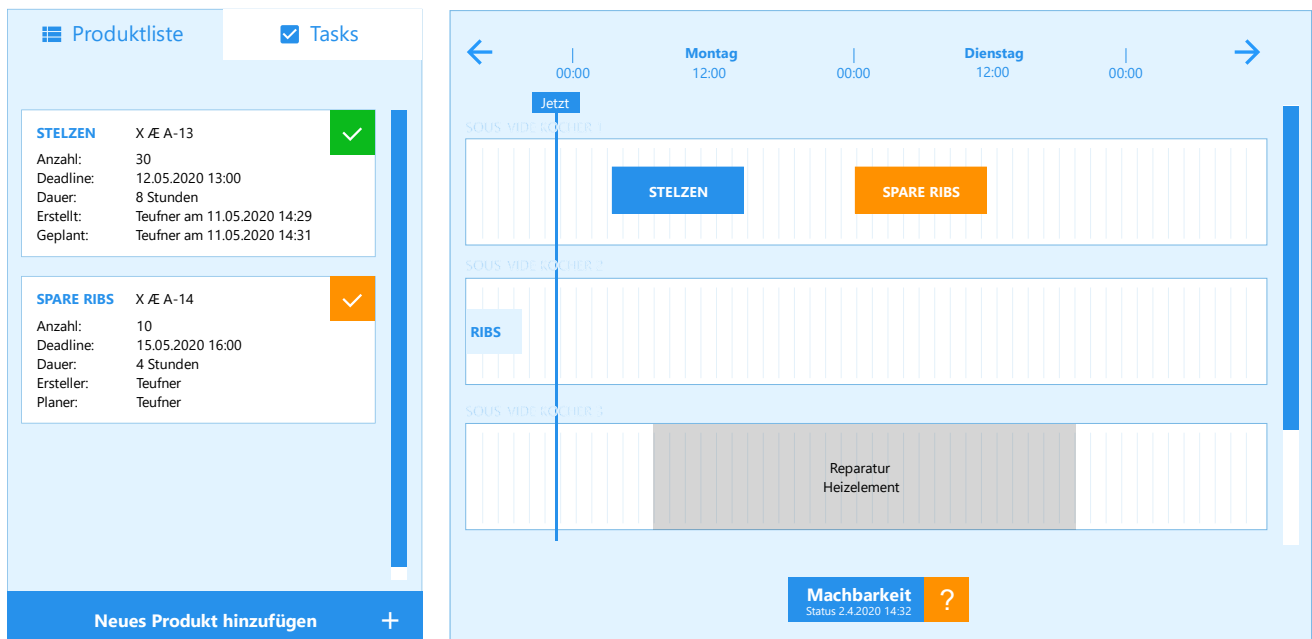


Figure 16: HMI concept of the plant operator of the production facilities (energy consumers)

EDCSProof Techniker

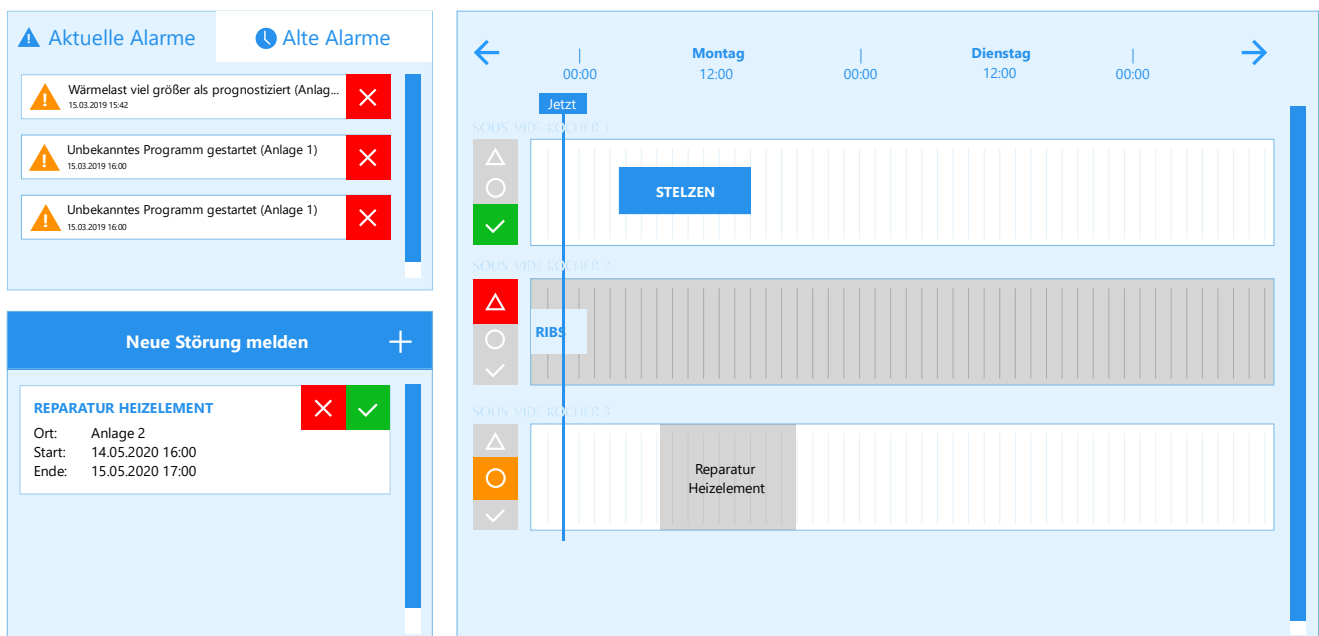


Figure 17: HMI concept of the technician

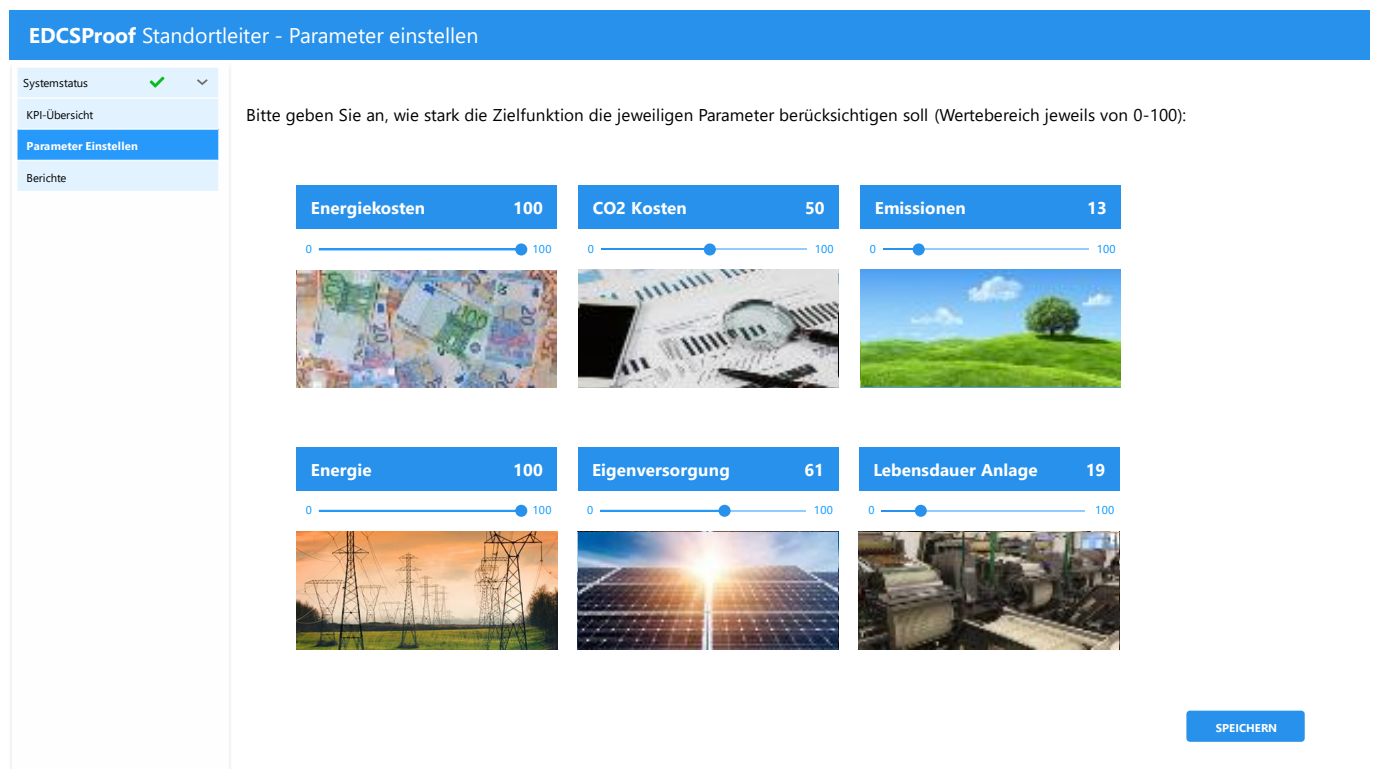


Figure 18: HMI concept of the manager: Setting parameters

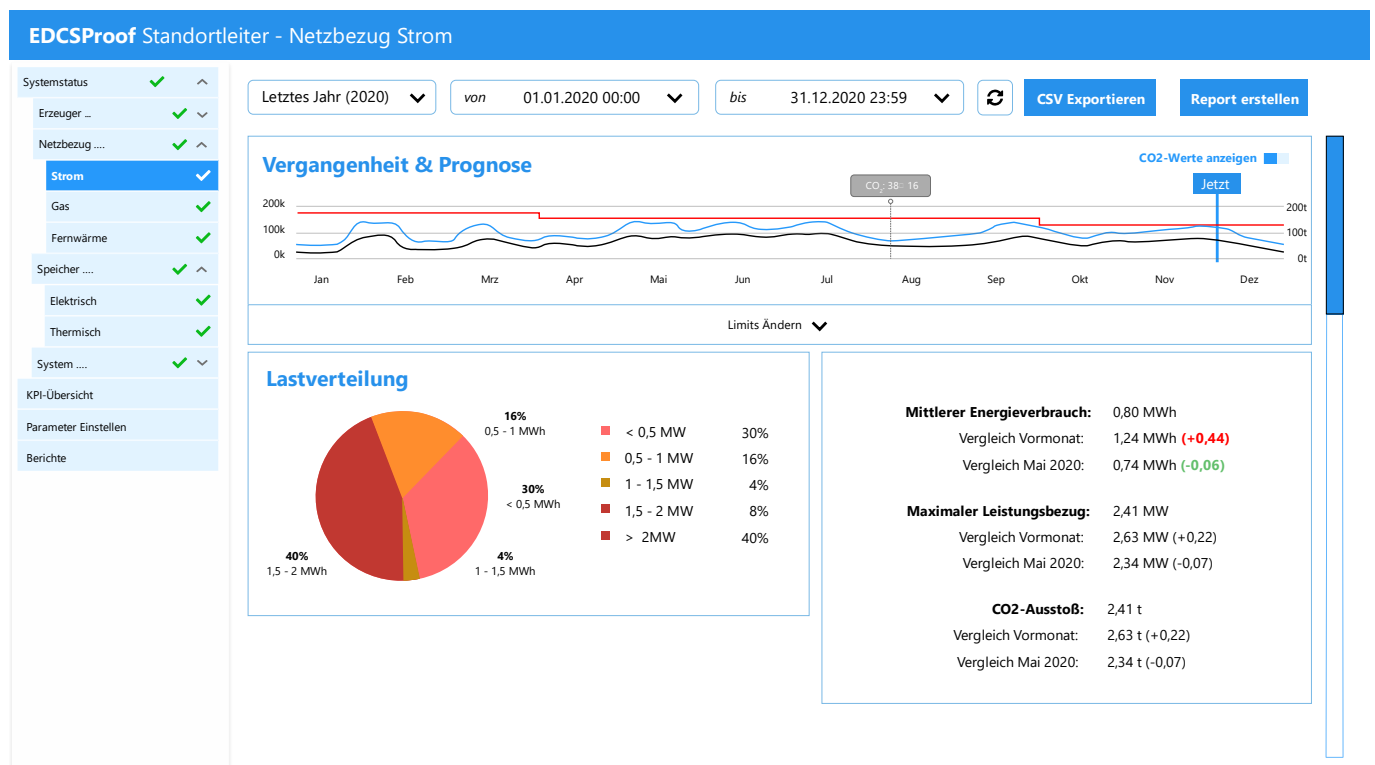


Figure 19: HMI concept of the manager: Electricity from the electricity grid

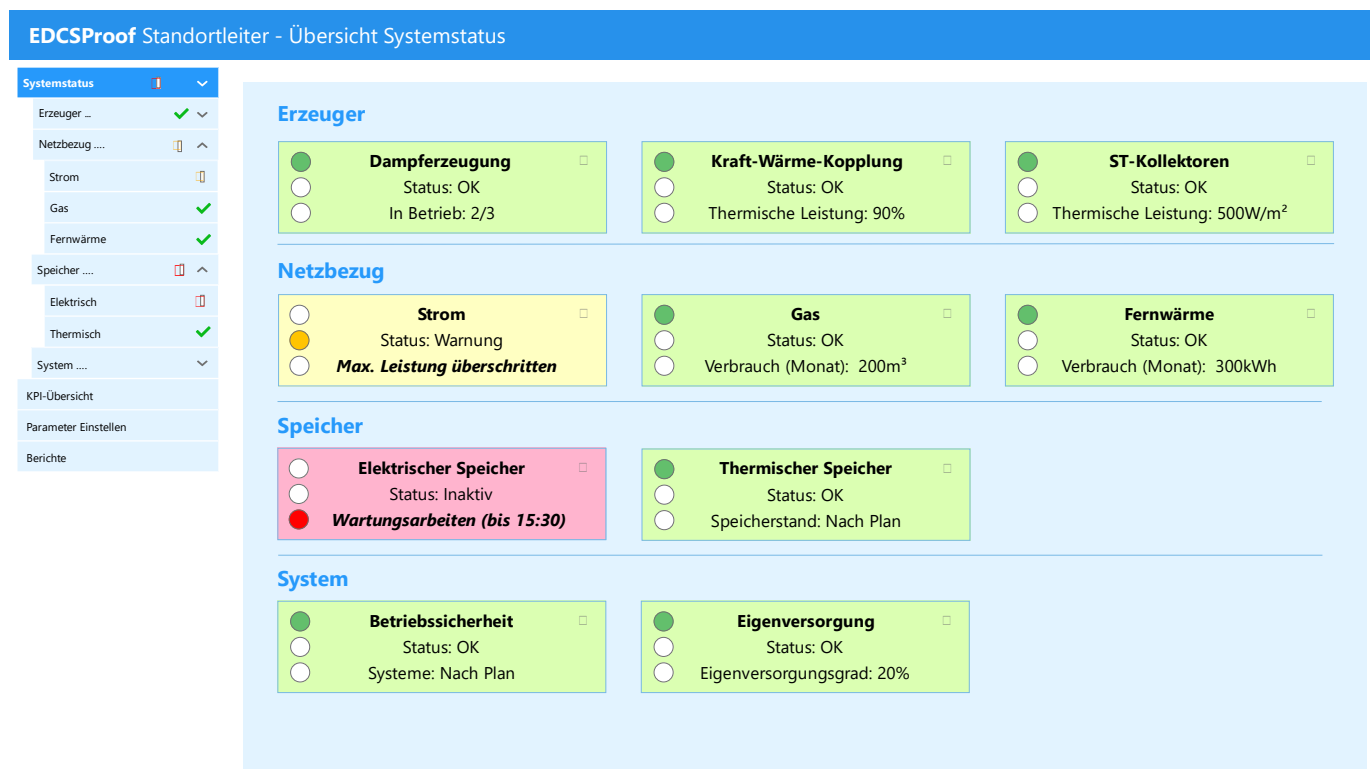


Figure 20: HMI concept of the manager: Overview system status

4.5. Performance of the EDCS in the laboratory

4.5.1. Introduction

Main goal of the laboratory experiments was to raise the technology readiness level (TRL) of the energy demand control system (EDCS, aka energy management system EMS) to level 4 'Validation in the laboratory'. Therefore, operating experience on representative operating scenarios had to be derived and optimization potential was detected. In the following, first the laboratory setup including the interface between the EDCS and the laboratory equipment is described followed by the operating scenarios. Then the results of the executed experiments are presented. These results were also published in a journal paper [9].

4.5.2. Laboratory setup

The schematic laboratory setup is shown in Figure 23, the control hardware architecture in Figure 21 and a laboratory impression in Figure 22. The setup was implemented in the laboratory's HP test bench, providing the heat source for the HP (blue rectangle) and a heat sink (red rectangle) to emulate the heat load. The setup consisted of three heat generators - a high temperature heat pump (HP), a boiler, and an electrical heater, as well as a water tank as thermal energy storage (TES). The energy management system (EMS=EDCS) was executed on a laptop (MATLAB® using the GUROBI solver) sending the controlled variables of the EMS (green) to a second laptop that executed XAMControl®. From here the values of the control variables of the underlying controllers were sent to the field layer.

FTI Initiative Energy Model Region - 1. Call for Projects

Federal Climate and Energy Fund – Handling by The Austrian Research Promotion Agency FFG

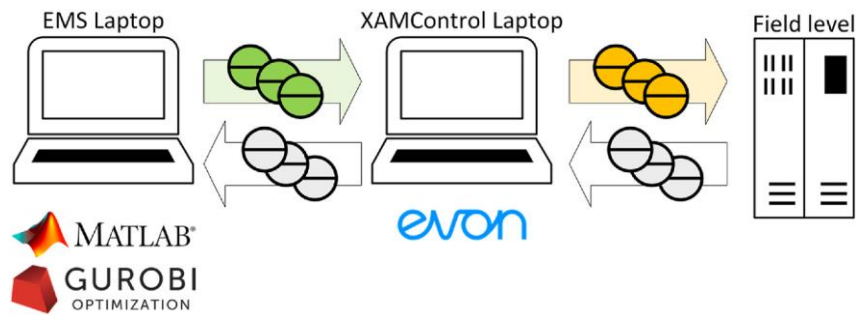


Figure 21: Control hardware architecture. Left: Laptop running the EMS on MATLAB using the GUROBI solver; Centre: Laptop running XAMControl® from the project partner evon; Right: Field level connecting to the laboratory setup from Figure 23. Circles: Green: Controlled values of the EMS; Orange: Control values of subordinate controllers; Grey: Measurement values.



Figure 22: Setup in the AIT heat pump laboratory with main components: Boiler (left, black), storage tank (centre, grey), three circulation pumps (green) with frequency converters, flow meters (blue), expansion vessels (red), tubes and pipes almost completely insulated.

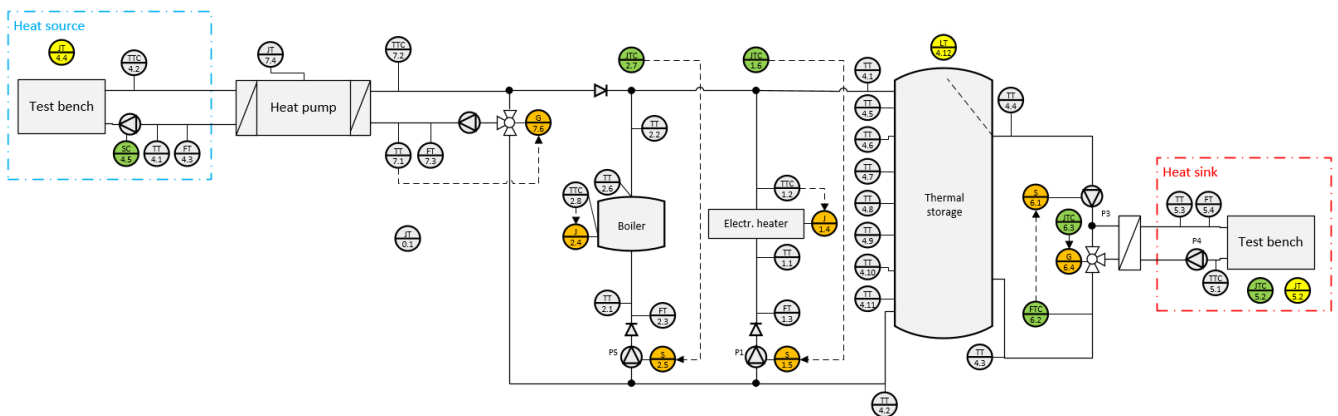


Figure 23: Schematic laboratory setup. The heat generators (heat pump, boiler, and electrical heater) charge the thermal storage to cover the demand (industrial load profiles). Green: Controlled values of the EMS; Orange: Control values of subordinate controllers; Grey: Measurement values; Blue: Heat demand (Disturbance).

4.5.3. Results

The laboratory setup was built and commissioned at the AIT HP laboratory. Overall, more than 30 experiments were executed. The experiments validated that the test rig could emulate industrial ESS and demonstrated the performance and robustness of the EMS for these setups. Two experiments with the setup experiment A and three experiments with the setup experiment B are presented in the following subchapters.

Operating scenario A

For operating scenario A, the performance of the EMS was compared to a standard hysteresis control. The trajectories of the significant measurements are displayed in Figure 24. Figure 24a shows the electricity price and the availability of the heat recovery system (HR). Figure 24b shows the result obtained with the hysteresis control. All available heat sources are turned on at the moment $T_{Hysteresis,on} = 60^{\circ}C$ is undercut and turned on when $T_{Hysteresis,off} = 70^{\circ}C$ is overshoot. The HP is used when its availability happens to coincide with activation – which is partly true for both availability periods. Overall, the hysteresis controller utilized 71.7% of the available HR. Further, it is visible that the hysteresis controller cannot guarantee production safety as the critical temperature is undercut at process time 556 minutes for 34 minutes. Such bottlenecks in the energy supply can impact product quality and cause high costs. Figure 24c shows that the EMS successfully prevents such bottlenecks in the heat supply. Further fully utilizes the HR by keeping the SOC low enough before HR availability periods. Overall, the SOC is kept at a low level to avoid temperature-dependent heat losses. The impact of the electricity price is also visible as the EMS does consume less power in the high price periods at the beginning and the end of the experiment.

By these measures, the EMS reduces the energy costs by 5.1% and reduces the CO₂ consumption by 9,2%. More detailed results can be found in Table 1.

Table 1: Control performance indicators for operating scenario A.

Case Study	Control	HR exploitation	Energy-Costs	CO ₂ emissions
A	Hysteresis	71.7%	4.14€	15.2.g/kWh
	EMS	100.00%	3.93€	13.8 g/kWh
	Saving	+28.4%	-5.1%	-9,2%

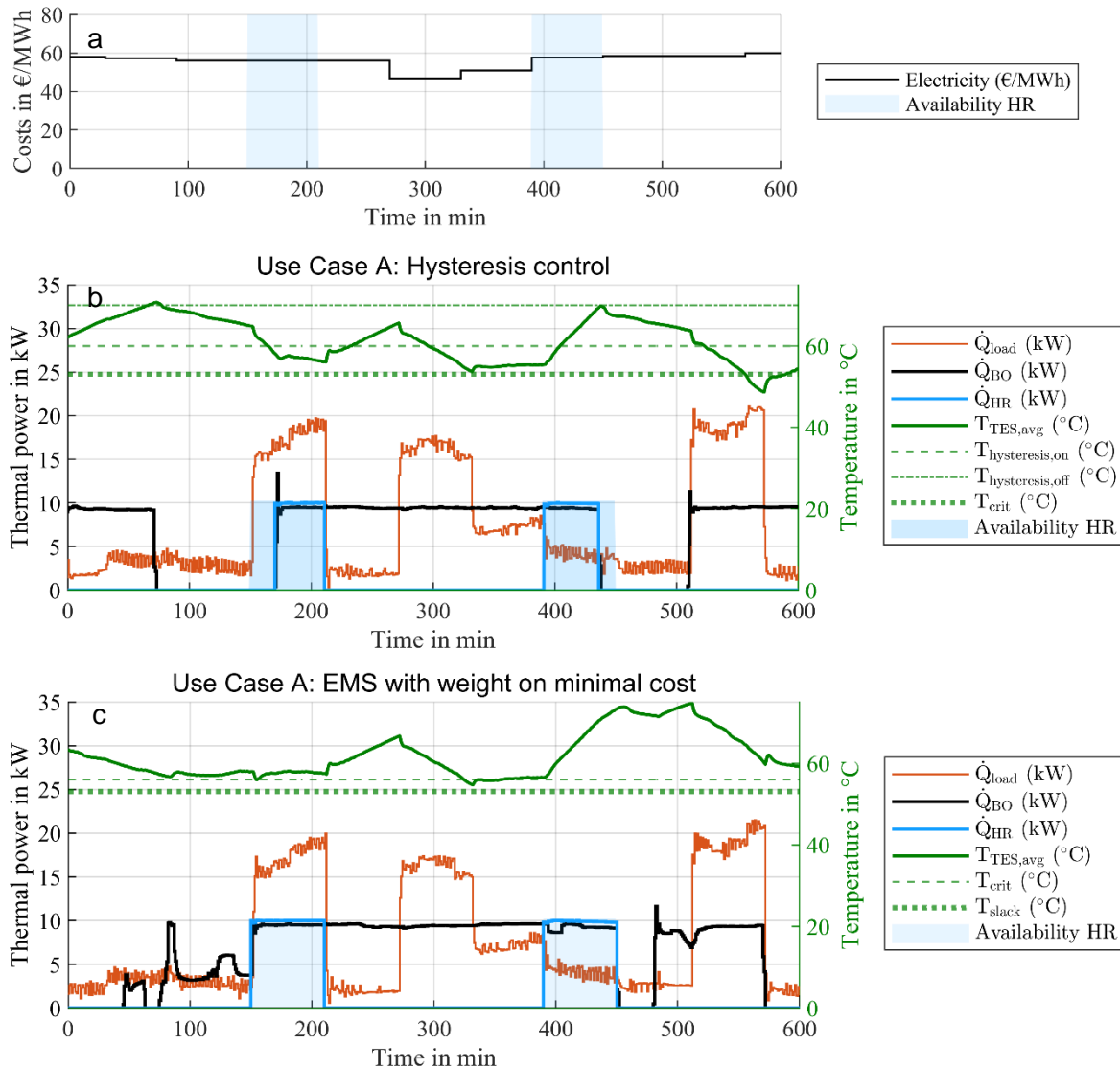


Figure 24 a-c: Measurements of operating scenario A where the energy supply system consists of an electric boiler BO, a temporary available heat recovery HR and a thermal energy storage TES. The performance of hysteresis control (b) is compared to the performance of the energy management system EMS (c).

Operating scenario B

For operation scenario B the performance of the EMS was compared to a standard hysteresis control for two different weight settings in the cost function. The trajectories of the important measurements are displayed in Figure 25a-d and the key performance indicators in Table 2. Figure 25a shows the electricity price, the availability of the HR, the availability of the HP and the CO₂ equivalent for both gas and power. The use case's goal was also to investigate the effort needed for adapting the EMS to a new configuration of components. It showed that the changes were done within minutes as a predefined modular HP model could be included and all parameters read from datasheets. The results are discussed for each control setting separately before they are compared.

Hysteresis control

All available heat sources are turned on at the moment $T_{Hysteresis,on} = 60^{\circ}C$ is undercut and turned on when $T_{Hysteresis,off} = 70^{\circ}C$ is overshoot. The disadvantage of non-predictive energy management is evident in HP utilization. The HP is used when its availability coincides with activation – even if it ends a few minutes later, as it happened at minute 90. Thereby high start-up-costs are caused without corresponding counter-value. Overall, the HP was exploited 50.8% of the time. Also, the HR was not fully exploited with 58.2%.

EMS optimizing costs

The EMS with weight on energy cost optimization fully exploited the HR. Further, it is visible that the EMS kept the SOC as low as possible to avoid losses. This, and the fact that producing heat with the gas boiler was cheaper in times the power price was high, caused that the HP was only exploited for 76.4%. The constantly low SOC and the model errors led to a violation of the soft constraint at minute 190 whereby the LLC increased the gas boiler utilization. Still, the EMS was always far from the critical low temperature and thereby caused no bottleneck in the energy supply.

EMS optimizing CO₂

The EMS with weight on CO₂ reduction fully utilized the HP due to the lower CO₂ equivalent of power than gas. Also, HR was fully exploited. The high usage of temporarily available heat sources led to a higher average SOC and heat losses.

Comparison

Table 2 shows the comparison between the three control strategies. The EMS is superior to the hysteresis control in all aspects. It is shown that temporarily available heat sources like HR or HP need a predictive control to unfold their potential fully. The different weights in the EMS cost function also showed the effect. Total weights on energy costs led to a cost reduction of 12.5%, while the optimization for CO₂ only decreased the cost by 2.4%. However, the EMS focused on CO₂ reduction decreased pollution by 41.8%, while the EMS optimizing cost only achieved a CO₂ reduction of 36.5% compared to the hysteresis control. The difference is caused by the utilization of the HP. While the EMS optimizing pollution utilized the HP also in times of high power cost - and thereby had a higher average SOC and heat losses to store the heat – the EMS optimizing cost preferred the gas boiler in times of high power prices.

Table 2: Control performance indicators for operating scenario B.

Control strategy	Control	HR exploitation	HP exploitation	Energy-Costs	CO ₂ emissions
B	Hysteresis	58.2%	50.8%	0.87€	10.31kg
	EMS optimizing costs	100.0%	76.3%	0.77€ / -12.2%	6.54 kg / -36.5%
	EMS optimizing emissions	100.0%	100.0%	0.85€ / -2.3%	6.00kg / -41,8%

FTI Initiative Energy Model Region - 1. Call for Projects

Federal Climate and Energy Fund – Handling by The Austrian Research Promotion Agency FFG

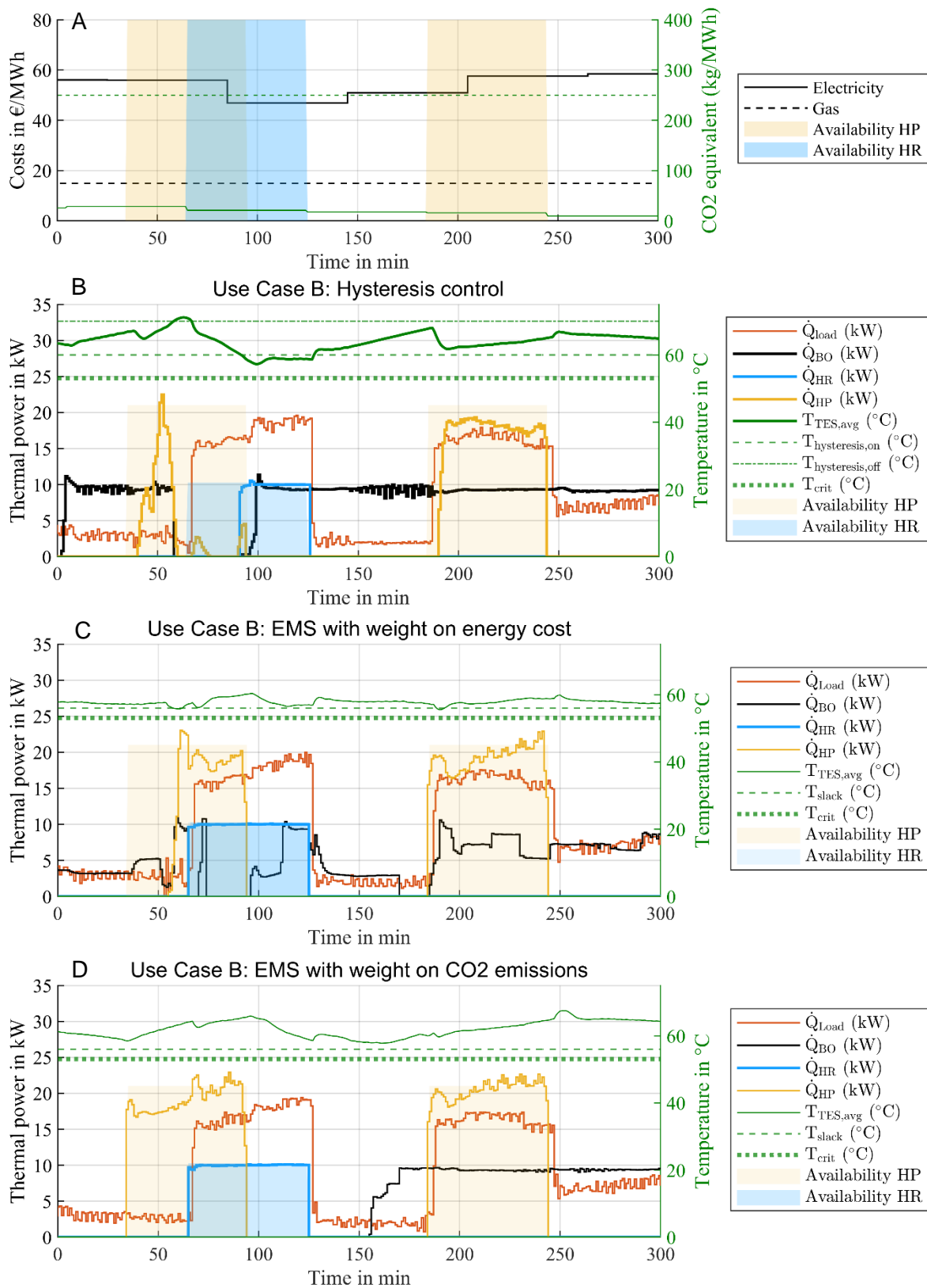


Figure 25 a-d: Measurements of operating scenario B where the energy supply system consists of a gas boiler BO, a temporary available heat recovery HR, a heat pump (HP) and a thermal energy storage TES. The performance of hysteresis control (b) is compared to the performance of the energy management system EMS with weight in energy cost (c) and to the performance of the energy management system EMS with weight on CO₂ emissions (d).

4.5.4. Conclusions

The main goal of the laboratory experiments - to raise the TRL of the EDCS to level 4 '*Validation in the laboratory*' – was successfully accomplished. Operating experience on representative operating scenarios were derived and optimization potential was detected. The benefits of the EDCS could be validated both qualitatively and quantitatively. Therefore, TRL4 was reached. The EDCS outperformed the benchmark controller in all experiments. Depending on the operating scenario a cost reduction of up to 12.2% and CO₂ reduction of 41.8% compared to the hysteresis controller were achieved. Substantial deviations of critical parameters can turn the measures of the EMS reduce the performance strongly but can easily be avoided with state-of-the-art parameter observers. Further the experience gathered during the experiments is extremely valuable for the further development of the EDCS.

4.6. Performance of the EDCSproof concept at the RES

The RES plant presented 4.4.1 was considered to evaluate the performance and savings potential of the EDCS in control of complex multi-energy system.

4.6.1. Approach

The study was executed based on the co-simulation procedure presented in Figure 26. As can be observed, the estimation of energy and cost savings that can be achieved by applying the predictive energy management and optimization system like the EDCS for the overall control of an industrial ESS is a manifold task. Moreover, it is highly dependent on the composition of the opposing energy system and the prevailing boundary conditions.

- Implementation of the EDCS in MATLAB
 - Mixed-Integer linear programming
- Simulation-model as a virtual representation of the plant
 - Detailed, non-linear component models, Matlab functions/FMUs

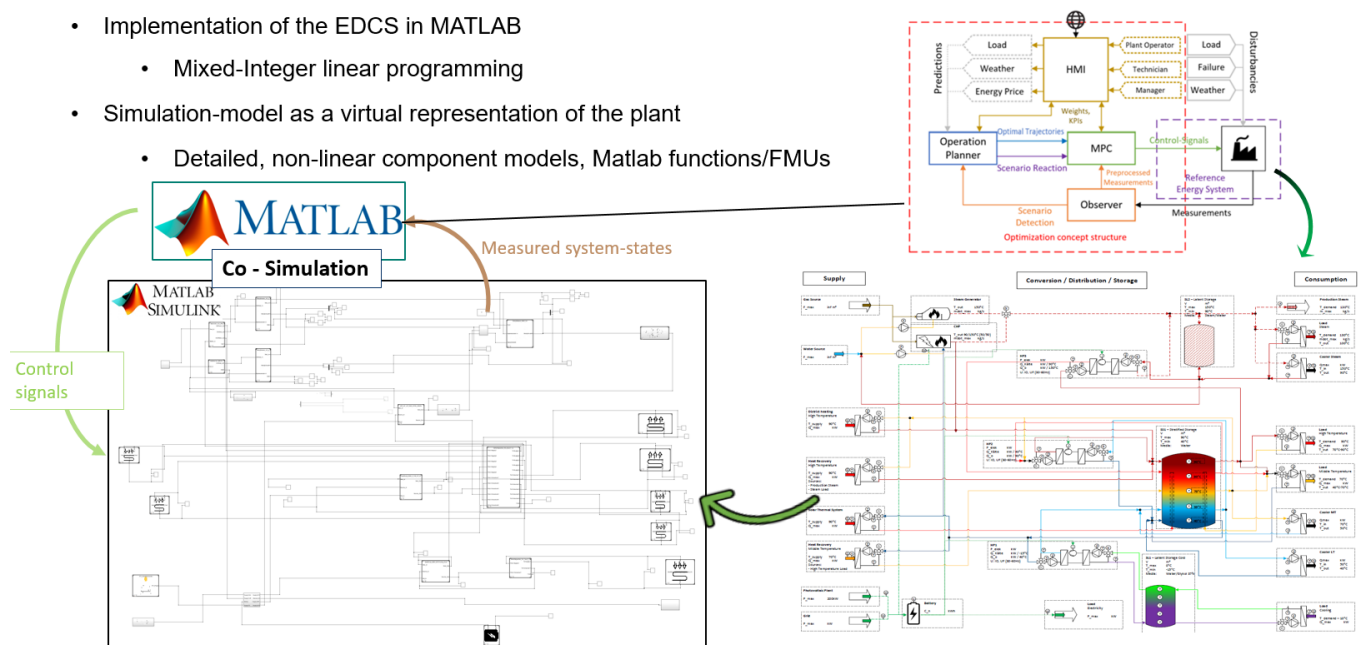


Figure 26: Co-Simulation Modelling Approach

The results depend very much on the specific boundaries imposed by energy markets, local climate and renewable generation capacity, accuracy of forecasts and the exploitable flexibility of the energy systems.

Also, the reference control concept, which is compared to the predictive and optimizing EDCS, has a very decisive influence on the investigation.

As illustrated in Figure 30, with the RES acting as use case in this evaluation, simulation studies for different scenarios (summer, winter, transition) were performed, where the controllable components of the energy systems were once controlled by the EDCS and a second time with a conventional 2-point controller(CC2P). The results of the different scenario simulations for both control cases and energy system versions were compared and interpreted to obtain general findings.

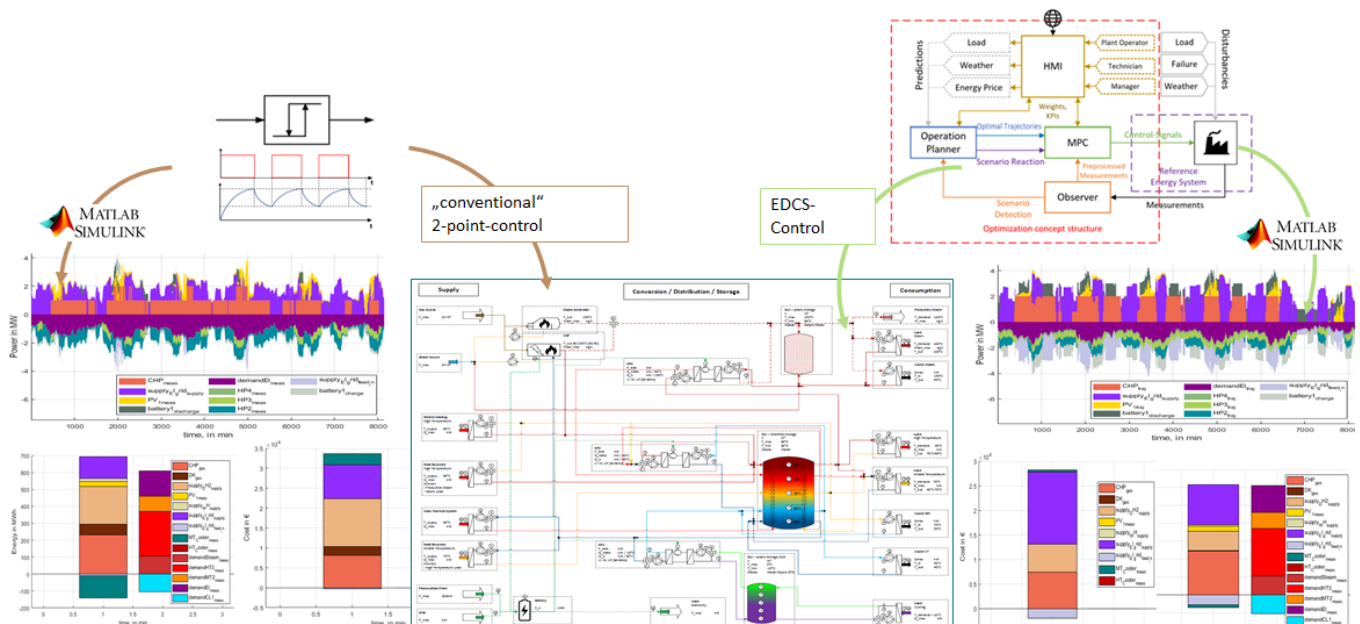


Figure 27: Comparison of an EDCS control vs. a conventional control method at the RES System

Figure 27 illustrates the comparison of an EDCS with a conventional rule-based control. Thereby clear differences in the operation trajectories of the two methods can be obtained. On the one hand, the different use of the individual components can be observed over time, and on the other hand, the savings in energy and costs.

4.6.2. Results

Figure 28 presents a high-level comparison of the different scenarios. It is apparent that an EDCS operation with the flexible system is always cost-optimal. Depending on the scenario overall energy savings up to 30% can be achieved and even more emissions and cost savings by an EDCS application. On the other hand, the effect of an EDCS application is low if only little flexibility is present. Also, investments in new low-carbon components, which would enable more flexibility, cannot exploit their full potential by using conventional control concepts. However, the full potential can be exploited through the application of a predictive and energy management and control concept like the EDCS.

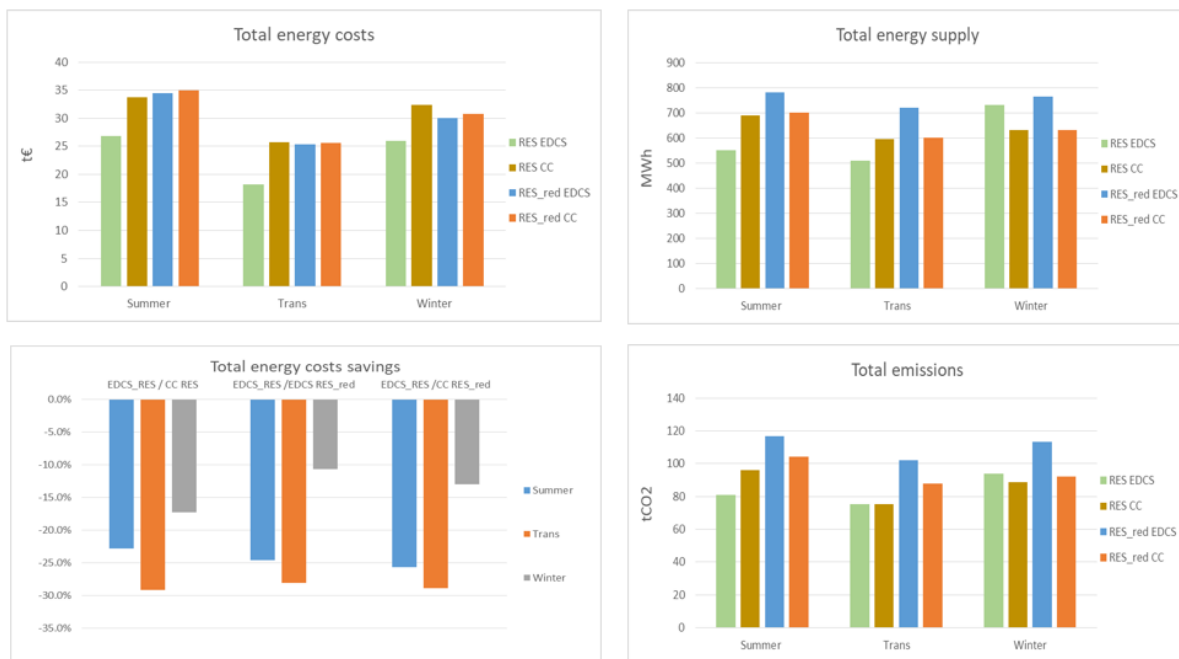


Figure 28: Overview of the estimated savings potentials at the RES plant for different scenarios

4.7. Performance of the EDCSproof concept at Wiesbauer Wien

The performance of the EDCSproof energy supply concept is presented for an evaluation by the example of the project partner Wiesbauer. Based on the analysis performed within the project (thermodynamical and exergetic analysis on historical process data) the location Wiesbauer Wien was identified as the most suitable location for the calculations regarding cost saving potential on an existing plant. The detailed investigations identified at Wiesbauer Wien the possibility to use low-temperature heating water in order to generate high temperature heating water by means of an additional water to water HP thereby reducing the steam demand (and thereby production).

As preliminary design parameters the following basis has been considered for all use case considerations:

- Integration of the HP in the area of the existing heat storage tanks
- Thermal capacity of the HP 350 kWth
- Primary side: supply temperature 50 °C / return temperature 35 °C
- Secondary side: supply temperature 90 °C / return temperature 65 °C

Based on the preliminary design parameters the integration of the new HP will be virtually implemented as simplified shown in the schematic drawing in Figure 29.

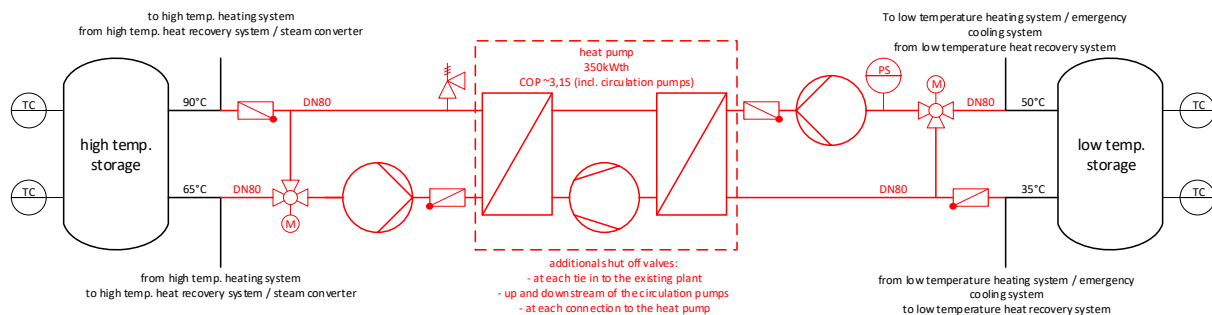


Figure 29: Simplified scheme of a heat pump integration at Wiesbauer Wien

The schematic integration is based on the typical data provided by reputable vendors of HPs. New dedicated circulation pumps ensure the transport of the medium from / to the two storage tanks. Motorized 3-way-valves on primary and secondary side are required in order to keep the inlet temperatures to the heat pump within the range which is specified by the vendor. Check valves are installed to ensure clear flow directions.

Based on the preliminary design it is expected that up to about 2,900 MW_{th} of natural gas (based on higher heating value) could be substituted.

4.7.1. Cost Calculation for the use case Wiesbauer Wien

In order to allow a more differentiated view on the optimization potential of the ECDSproof system for the use case the cost estimation has been divided in following 2 parts:

- Cost estimation for integration of the HP
- Cost estimation for integration of ECDS control system

This approach allows to investigate following 4 different cases instead of 2:

- Base Case (current status no changes)
- Base Case + EDCS
- Base Case + HP
- Base Case + HP+ EDCS

4.7.2. Cost calculation for the heat pump integration

Due to the fact that the design parameters are only preliminary the cost estimation that has been performed at this stage is also based on certain assumptions. These assumptions have to be verified during detail-engineering phase after the final design parameters are fixed. To minimize the uncertainty of the overall cost estimation an indicative price inquiry for the HP package (represents approximately 50 % of the total invest cost) has been performed. Other costs have been calculated based on “in house” data bases and engineering experience of the project partner ILF. The results of the cost calculation for the integration of the HP can be found in Table 3. For the implementation of the HP a project duration of about 7-9 months is expected.

Table 3: Cost estimation for a heat pump integration at Wiesbauer Wien

Position	Cost [kEUR]	Source	Uncertainty	Comments
Heat pump package	149	OEM	+/- 15%	Heat pump including control cabinet, primary and secondary circulation pumps, shut off valves, check valves, strainer, safety valve for secondary side, compensator, commissioning
Civil	10	ILF	+/- 50%	Vibration damping foundation (assumption: sufficient spare space for installation in an existing boiler room as well as sufficient spare capacity in existing HVAC system available)
Electrical, instrumentation and control	14	ILF	+/- 50%	Integration and adaption of existing control system, electrical connection and cabling (assumption: sufficient power reserves and reserve for outgoing feeder as well as on existing cable routes available; main supply distance max. 50m, supply to pumps and valves max. 10m)
Piping and mechanical erection	65	ILF	+/- 50%	Pipe DN80, coating and insulation as well as installation of heat pump package (assumption: max. 50m distance to each of the 4 tie in points; sufficient spare reserves on existing pipe racks)
Engineering	59	ILF	+/- 50%	Including approval planning, documentation, training; excluding owner's cost.
Overall Invest	279		+/- 27%	According to weighted uncertainty

Table 4: Cost estimation for the EMS integration at Wiesbauer Wien

Position	Cost [kEUR]	Source	Uncertainty	Comments
Hardware	10	OEM/ILF	+/- 20%	Hardware control unit, additional equipment for connection to inventory control system
Integration	8	OEM/ILF	+/- 20%	Engineering / integration of EDCS control system into existing station control system
Engineering OEM	10	OEM/ILF	+/- 10%	Engineering by OEM for integration of existing station control system
Engineering EDCS	30	OEM/ILF	+/- 50%	Project specific programming of EDCS control system
Miscellaneous	5	OEM/ILF	+/- 30%	Commissioning, documentation, training, spare parts
Overall Invest	63		+/- 34%	According to weighted uncertainty

Table 5: Cost estimation for the running costs of the EDCS control system

Position	Cost [kEUR]	Source	Uncertainty	Comments
Fees	20	OEM/ILF	+/- 50%	Expected annual fees for EDCS control system

Table 6: Operational costs and savings for different execution stages at Wiesbauer Wien

	Operational Cost [kEUR/a]	Savings to Base Case [kEUR/a]	Savings to Base Case [%]
Base Case	1,553	0	0%
Base Case + EDCS	1,530	23	≈1.5%
Base Case + HP	1,504	49	≈3.2%
Base Case + HP+ EDCS	1,407	86	≈5.5%

4.7.1. Cost calculation for the EMS integration

The cost estimation for the integration of the energy management system (i.e., the EDCS control system) shown in Table 4 is based on OEM prices as well as “in house” data bases and engineering experience of the project partner ILF. For the integration of the EDCS a project duration of about 3-4 months is expected. The EDCS control system is expected to have annual fees shown in Table 5.

4.7.2. Economic Analysis

For the use case Wiesbauer Wien a static amortization time based on the following economical parameters has been performed:

- Natural gas price: 35 €/MWh (higher heating value)
- Price for electricity: 100 €/MWh
- Cost for CO₂: 40 €/t (0,2 t_{CO2}/MWh)
- Utilization rate for conventional heat generation: 80% (higher heating value)

As a limit for the static amortization time a limit of 10 years has been defined.

Table 6 shows the operational costs and annual savings. It can be seen that there is a relationship between the complexity of a system and the potential of energy saving by means of the EDCS system. An implementation of only the EDCS for the base case would lead to yearly annual savings of about 1.5%. The integration of the EDCS in the more complex system which also comprises the new HP would boost the savings by 2.3% instead of 1.5% from about 3.2% to approximately 5.5% in comparison to the base case. In comparison to the base case the “efficiency” of the EDCS is increased by more than 50%.

The investment for the use case (comprises of the integration of the new heat pump as well as for the installation and operation of the EDCS system) has a static amortization time of 5.5 years which is nearly half the time which has been defined as the limit.

4.7.3. Conclusion

The calculations, simulations and research work carried out for the use case Wiesbauer Wien show that the integration of the EDCSproof concept as both the EDCS controller and a HP is economically beneficial in a moderate static amortization time. There is the clear suggestion to implement this concept at Wiesbauer Wien.

4.8. Applicability of the EDCSproof concept in other industries

Within the project analyzes were carried out regarding the applicability of the EDCSproof concept in other industrial sectors. The target was not a detailed analysis, but an overview over factors like complexity, cost- and customer variability, possible excess capacities, continuity of the process as well as variety of different energy sources within the different industries, that can be seen as indicators for optimization potential. The results are summarized in Table 7 to give an overview over the potentials of the different sectors.

Table 7 Summary of potential for the application of the EDCSproof energy supply concept

	Power	Food and Beverages	Construction Materials	Pharma	Pulp and Paper	Plastics	Textiles	Metal
Complexity	+	+	~	+	+	+	~	~
Excess Capacities	+	+	+	+	~	~	-	~
Variable Cost	+	+	+	+	~	+	+	+
Variable Customers	+	~	+	+	~	+	+	+
Discontinuous Processes	+	~	~	+	-	~	~	~
Different Energy Sources/ Consumers	+	+	+	+	+	+	+	+
+ high potential, ~ medium potential, - low potential								

It is clearly visible that the majority of the factors can be evaluated positively in terms of potential for improvements, which shows the broad applicability of the EDCSproof energy system.

Furthermore, all of the discussed industrial sectors are expected to grow in the near future, while also being subject of continuous improvements that are necessary on the path towards a sustainable future. Thus, the application of approaches like EDCSproof is not only possible, but necessary in most industrial sectors.

5. Outlook and recommendations

As shown in Figure 30 the development timeline of the EDCSproof optimal controller is defined until the stage of a start-up or spin-off on TRL 8. Results of EDCSproof are used and further developed in the follow-up project “Industry4Redispatch” (3rd Call – Energy Model Region), led by AIT, to lift the TRL to 7 (esp. controller and HMI). Aim of Industry4Redispatch is the control of industrial energy supply systems to make optimal use of flexibilities. In the project all relevant stakeholders work together to develop both systemic and technical solutions for the industrial energy system. 7 of the 9 project partners of EDCSproof are consortium members in the follow-up project.⁵

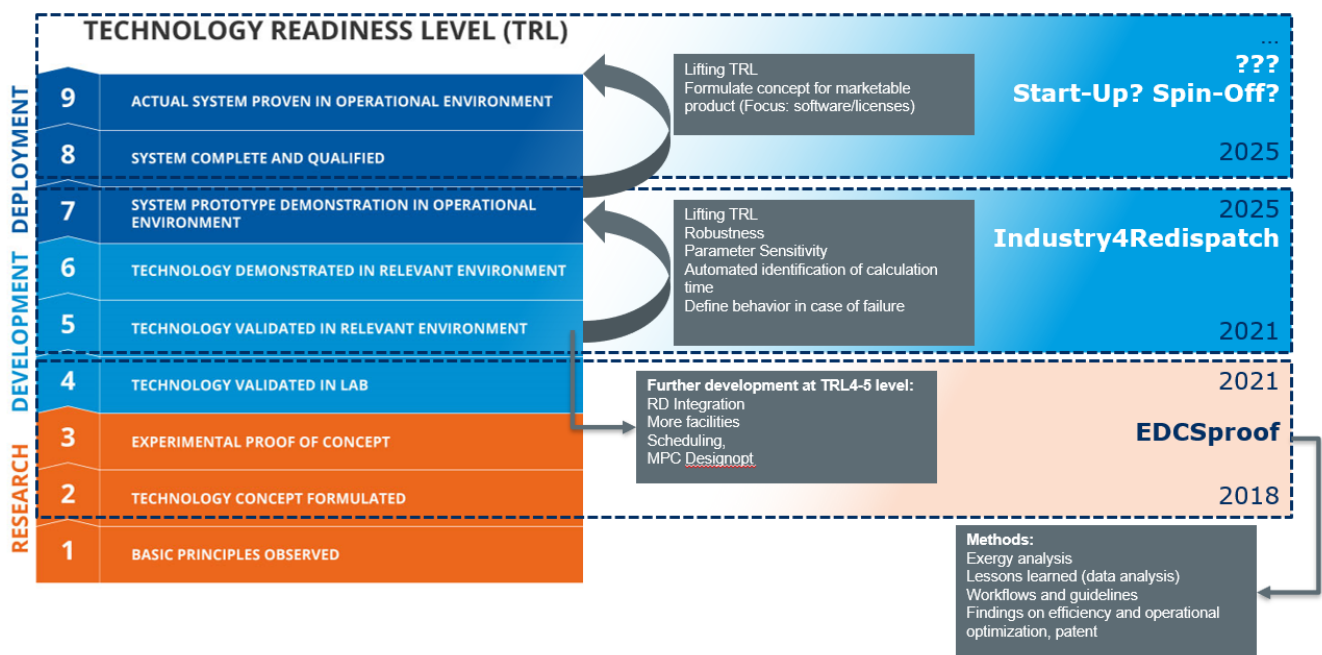


Figure 30: Development timeline of the EDCSproof concept

Within EDCSproof a patent was filed at Österreichisches Patentamt with no. A 60058/2022 by ARPA, IET, AIT, and evon GmbH to design the configuration and the operation of a model-predictive and optimal energy controller within a process control system with as little effort and as automatic as possible. This enables beneficial exploitation by the partners. The latent heat storage developed within EDCSproof will be further used in the NEFI project envloTcast⁶ with a long-term durability test of the storage, beginning at the AIT thermal storage lab.

Recommendations from EDCSproof:

- Push digitalization to improve availability of measurement data as basis for decarbonization measures. This enables simulation models and demand forecasts to be more accurately.
- Improve framework of state subsidies for implementation of concepts like EDCSproof
- Push connectivity of components (supply, storages, consumers) with standardized protocols (e.g., OPC UA) to enable concepts like EDCSproof to control the whole plant in an optimal way.
- Pricing of greenhouse gas emissions will push industry to invest in concepts like EDCSproof.

⁵ <https://nefi.at/en/project/industry4redispatch>

⁶ <https://nefi.at/en/project/enviotcast>

6. Bibliography

- [1] M. Thombre, Z. Mdoe and J. Jäschke, “Data-driven robust optimal operation of thermal energy storage in industrial clusters,” *Processes*, vol. 8, no. 2, 2020.
- [2] G. Schmid, M. Lauermann, M. Hartl, V. Wilk and A. Hafner, “Butan als Kältemittel für Wärmepumpen in industriellen Prozessen,,” in *DKV-Tagung 2015, 18.-20.11.2015*, Dresden, 2015.
- [3] C. Zauner, B. Windholz, M. Lauermann, G. Drexler-Schmid and T. Leitgeb, “Development of an Energy Efficient Extrusion Factory employing a latent heat storage and a high temperature heat pump,” *Applied Energy*, vol. vol. 259, 2020.
- [4] C. Schlemminger, C. Kopp, K. Banasiak, G. Drexler-Schmid, M. Lauermann, B. Windholz, C. Zauner and A. Baumhake, “Hochtemperatur Wärmepumpe mit Ejektor,” in *DKV-Tagung 2019, 20.-22.11.2019*, Ulm, 2019.
- [5] I. H. Bell, J. Wronski, S. Quoilin and V. Lemort, “Pure and Pseudo-pure Fluid Thermophysical Property Evaluation and the Open-Source Thermophysical Property Library CoolProp,” *Industrial & Engineering Chemistry Research*, vol. 53, no. 6, pp. 2498-2508, 2014.
- [6] S. Elbel and N. Lawrence, “Review of recent developments in advanced ejector technology,” *International Journal of Refrigeration-Revue Internationale Du Froid*, pp. 1-18, 62 2016.
- [7] F. Fuhrmann, A. Schirrer, M. Kozek and S. Jakubek, “Prediction of pulsed heat loads in manufacturing plants,” in *IFAC World Congress 2020*, online, 11.-17.7.2020.
- [8] F. Fuhrmann, A. Schirrer and M. Kozek, “MPC for Process Heat Supply Systems : Considering load prediction uncertainty caused by human operators,” in *Proceedings of the 30th European Symposium on Computer Aided Process Engineering (ESCAPE30)*, Milano, Italy, May 24-27, 2020.
- [9] F. Fuhrmann, B. Windholz, A. Schirrer, S. Knöttner, K. Schenzel and M. Kozek, “Energy management for thermal batch processes with temporarily available energy sources– Laboratory experiments,” *Case Studies in Thermal Engineering*, no. 102473, 2022.

7. Appendix

Table 8: Heat output and second-law efficiency as well as further data of the heat pump on Figure 5 and Figure 6

Heating capacity	Sink outlet temperature	Sink heating	Super-heating at evaporator	Super-heating suction gas	Super-heating hot gas	Source inlet temperature	Source outlet temperature	Second-law efficiency
kW	°C	K	K	K	K	°C	°C	-
25,2	97,4	10,0	8,6	20,6	14,4	49,5	34,8	0,39
25,5	98,3	10,0	8,0	20,9	14,2	50,2	35,4	0,39
25,5	98,9	9,9	8,4	21,2	13,8	50,7	35,7	0,38
25,9	97,6	10,0	7,2	21,6	14,3	51,7	36,3	0,38
26,0	100,8	10,1	8,2	20,1	13,2	52,1	36,9	0,38
26,2	101,7	9,8	9,1	19,4	12,8	52,3	37,1	0,38
26,4	102,9	9,9	9,6	19,6	12,7	52,6	37,3	0,38
27,7	108,9	30,0	11,3	21,7	15,7	46,9	43,6	0,41
28,5	112,6	30,0	12,5	21,4	15,1	49,8	46,5	0,41
30,3	106,8	10,0	8,4	20,8	15,2	51,0	40,5	0,41
30,4	112,2	15,0	8,5	20,2	14,8	51,0	41,0	0,41
30,9	107,5	10,0	8,2	21,2	15,4	51,2	40,7	0,42

8. Contact details

Bernd Windholz, **AIT – Austrian Institute of Technology GmbH**

Giefinggasse 2, 1210 Vienna

T: +43 664 2351933 F: +43 50550-6679

bernd.windholz@ait.ac.at

www.ait.ac.at

www.nefi.at/en/project/edcsproof

René Hofmann, **Technische Universität Wien, Institut für Energietechnik und Thermodynamik**

Alexander Schirrer, **Technische Universität Wien, Institut für Mechanik und Mechatronik**

Thomas Kienberger, **Montanuniversität Leoben, Lehrstuhl für Energieverbundtechnik**

Andreas Leitner, **evon GmbH**

Christopher Binder, **ILF Consulting Engineers Austria GmbH**

Magdalena Teufner-Kabas, **kleinkraft OG**

Reinhard Teufner, **Wiesbauer Holding AG**

Markus Siedl, **Fischer Brot GmbH**